Journal of Computational Physics 229 (2010) 2964–2998

Contents lists available at ScienceDirect

Journal of Computational Physics

journal homepage: www.elsevier.com/locate/jcp

Modeling phase transition for compressible two-phase flows applied to metastable liquids

Ali Zein *, Maren Hantke, Gerald Warnecke

Institute for Analysis and Numerics, Otto-von-Guericke-University Magdeburg, PSF 4120, D-39106 Magdeburg, Germany

ARTICLE INFO

Article history:
Received 14 July 2009
Received in revised form 16 December 2009
Accepted 18 December 2009
Available online 4 January 2010

Keywords:
Two-phase flow
Compressible flow
Phase transition
Relaxation
Six-equation model
Seven-equation model

ABSTRACT

The seven-equation model for two-phase flows is a full non-equilibrium model, each phase has its own pressure, velocity, temperature, etc. A single value for each property, an equilibrium value, can be achieved by relaxation methods. This model has better features than other reduced models of equilibrium pressure for the numerical approximations in the presence of non-conservative terms. In this paper we modify this model to include the heat and mass transfer. We insert the heat and mass transfer through temperature and Gibbs free energy relaxation effects. New relaxation terms are modeled and new procedures for the instantaneous temperature and Gibbs free energy relaxation toward equilibrium is proposed. For modeling such relaxation terms, our idea is to make use of the assumptions that the mechanical properties, the pressure and the velocity, relax much faster than the thermal properties, the temperature and the Gibbs free energy, and the ratio of the Gibbs free energy relaxation time to the temperature relaxation time is extremely high. All relaxation processes are assumed to be instantaneous, i.e. the relaxation times are very close to zero. The temperature and the Gibbs free energy relaxation are used only at the interfaces. By these modifications we get a new model which is able to deal with transition fronts, evaporation fronts, where heat and mass transfer occur. These fronts appear as extra waves in the system. We use the same test problems on metastable liquids as in Saurel et al. [R. Saurel, F. Petitpas, R. Abgrall, Modeling phase transition in metastable liquids: application to cavitating and flashing flows, J. Fluid Mech. 607 (2008) 313–350]. We have almost similar results. Computed results are compared to the experimental ones of Simões-Moreira and Shepherd [J.R. Simões-Moreira, J.E. Shepherd, Evaporation waves in superheated dodecane, J. Fluid Mech. 382 (1999) 63–86]. A reasonable agreement is achieved. In addition we consider the six-equation model with a single velocity which is obtained from the seven-equation model in the asymptotic limit of zero velocity relaxation time. The same procedure for the heat and mass transfer is used with the six-equation model and a comparison is made between the results of this model with the results of the seven-equation model.

1. Introduction

In the last two decades, considerable research has been devoted to the modeling and simulation of compressible two-phase flows. Most of the models used are typically derived by using averaging procedures [9,10,14]. Both the mathematical modeling and numerical computation have certain inherent difficulties.

* Corresponding author. Tel.: +49 3916711992; fax: +49 3916718073.
E-mail addresses: ali.zein@ovgu.de (A. Zein), maren.hantke@ovgu.de (M. Hantke), warnecke@ovgu.de (G. Warnecke).

0021-9991/$ - see front matter © 2009 Elsevier Inc. All rights reserved.
doi:10.1016/j.jcp.2009.12.026

The difficulties in modeling concern the physical transfer processes taking place across the interface such as mass, momentum and heat transfer. Using averaging techniques of the single phase equations results in additional terms, which describe these transfer processes. The exact expressions for the transfer terms are usually unknown [9]. Also there appear differential terms that are extracted from the transfer terms that prevent the system from being in divergence form. Therefore, they are referred to as the non-conservative terms and they are responsible for numerical difficulties.

The most general two-phase flow model consists of seven partial differential equations, the evolution equation for the volume fraction of one of the phases together with balance equations for mass, momentum and energy for each phase. The seven-equation model is a full non-equilibrium model, each phase has its own pressure, velocity, temperature, etc. Several authors considered such type of models, Baer and Nunziato [4], Embid and Baer [11] as well as Saurel and Abgrall [27]. Saurel and Abgrall [27] proposed a Godunov-type method for the solution of this model. Also they proposed instantaneous relaxation procedures for the pressure and the velocity that make the pressures and velocities of phases relax to common values. The main disadvantage of this model is the large number of waves.

Several authors have considered a five-equation reduced model which is obtained in the asymptotic limit of the seven-equation model, see Kapila et al. [15], Murrone and Guillard [23], Petitpas et al. [24] and Saurel et al. [33]. This model satisfies the mechanical equilibrium, it has a single pressure and a single velocity. It is composed of two mass equations, a mixture momentum equation and a mixture energy equation. These equations are written in conservative formulation, while the fifth-equation of this model is a non-conservative equation for the volume fraction which contains a non-conservative term involving the divergence of the velocity.

Even though the five-equation model is reduced it has severe numerical difficulties. These difficulties include:

- Shock computational difficulties due to the non-conservative character of the model.
- Maintaining volume fraction positivity due to the difficulties in the approximation of the non-conservative term involving the divergence of the velocity.
- Non-monotonic behavior of the mixture sound speed, that obeys the Wood formula, with respect to the volume fraction, see [34]. This behavior may cause inaccurate wave transmission across diffuse interfaces.

The above difficulties are detailed in Saurel et al. [34] and Petitpas et al. [24]. It is noted that the conventional Godunov-type schemes are not suitable for the resolution of this model [24]. To circumvent these difficulties, the Riemann problem is solved by the help of shock and Riemann invariant relations that were derived by Saurel et al. [32]. And a specific relaxation projection method is used instead of the conventional Godunov method, see Saurel et al. [29] and Petitpas et al. [24]. Moreover, Saurel et al. [33] modified this model to take into account phase transition by including temperature and chemical potential relaxation effects.

From the computational point of view the seven-equation model has several advantages over the five-equation model:

- Preserving the positivity of the volume fraction is easier.
- The mixture sound speed has a monotonic behavior, see Petitpas et al. [24].

According to the attractive advantages of the seven-equation model we aim in this paper to modify this model to include the heat and mass transfer and to present numerical investigations for the resulting model compared with some previously known results. Our attention is devoted to the evaporation that appears in cavitating flows. Thus we can compare our results with the results of Saurel et al. [33] for metastable liquids, i.e. liquids with temperature higher than the saturation temperature.

We use the seven-equation model of Saurel and Abgrall [27] which is a modified form of the Baer–Nunziato model [4]. For the solution of the hyperbolic part of the model a modified Godunov-type scheme is used. For the mechanical relaxation, the instantaneous velocity and pressure relaxation procedures of Saurel and Abgrall [27] are taken.

We insert the heat and mass transfer through relaxation effects. New terms associated with the heat and mass transfer are modeled, these terms are given in terms of the temperature difference for the heat transfer and in terms of the Gibbs free energy difference for the mass transfer. Also we propose new procedures for the instantaneous temperature and Gibbs free energy relaxation toward equilibrium. These procedures are used at each time step after the mechanical relaxations. They are used only at specific locations, i.e. at evaporation fronts.

Since the exact expressions for the transfer terms are unknown, our idea to model them is to refer to some general physical observations besides the second law of thermodynamics. In particular we assume that the mechanical properties relax much faster than the thermal properties. Also we assume that the relaxation time for the temperature is much smaller than that of the Gibbs free energy. In fact these assumptions agree with physical evidence in a large number of situations, see [5,13,15,22]. In the book of Müller and Müller [22] some similar assumption is used in the analysis of the equilibrium conditions for droplets and bubbles, see Chapter 11 there. In Kapila et al. [15] there are some estimates given for the time scales of the relaxation of the velocity, pressure and temperature in granular materials. These estimations show that the relaxation time for the temperature is significantly larger than relaxation times for both the velocity and the pressure. Also other estimations for detonation applications show that the time scale of the velocity relaxation and pressure relaxation are of the same order of magnitude while the temperature relaxation time is much greater than that for the velocity and pressure, see [7,26]. More discussion of this point is given in Section 3.2.

By our modifications of the seven-equation model we get a new model which is able to deal with transition fronts, specifically here evaporation fronts, where heat and mass transfer occur. These fronts appear as extra waves in the system, see Le Metayer et al. [21] and Saurel et al. [33].

Moreover we consider the six-equation model with a single velocity which is obtained from the seven-equation model in the asymptotic limit of zero velocity relaxation time. This model consists of the volume fraction equation of one of the phases, two mass balance equations, a mixture momentum equation and two energy equations. As with the seven-equation model this model has better features for numerical computations than the five-equation model. In fact the major difficulty in the numerics of the five-equation model comes from the equilibrium of the pressure. For more details concerning the six-equation model without phase transition you can see [34].

We model the heat and mass transfer for the six-equation model by using our procedure that is proposed for the seven-equation model under the same assumptions.

We use the same test problems of Saurel et al. [33] for metastable liquids. We see in our results the extra waves that appear due to the phase transition. Also our results are in a good agreement with the results of Saurel et al. [33].

Computed results are compared to the experimental data of Simões-Moreira and Shepherd [36]. Indeed, the computed front velocities of the evaporation waves are compared to the measured ones at several initial temperatures. There is a reasonable agreement with the experimental data.

A comparison between the results of the two models is made. There is no significant difference between the results of both models under the same conditions, but there is a significant difference in the CPU time consumed by both models, this makes the six-equation model less expensive.

This paper is organized as follows: In Section 2 we present the mathematical model and its closure relations. Also we deduce phasic entropy equations that will be used in later sections. Section 3 is devoted to the numerical method, in particular, we present a modified Godunov-type scheme with the HLLC-type Riemann solver [38] for the seven-equation model. In Section 4 we model the heat and mass transfer through the temperature and the Gibbs free energy relaxation effects. Our modeled terms keep the mechanical equilibrium during the temperature relaxation, also they keep the mechanical equilibrium and the temperature equilibrium during the Gibbs free energy relaxation. Mathematical procedures are introduced for the instantaneous relaxation of the temperature and the Gibbs free energy that are used at each time step after the velocity and the pressure relaxation. In Section 5 we consider the six-equation model with a single velocity, we apply the same ideas proposed for the heat and mass transfer in the seven-equation model on this case too. Finally, in Section 6 we present some numerical results. Comparison with experimental data is made and comparisons between the results of the seven-equation model and the six-equation model are considered.

2. Mathematical model

The two-phase flow model of Saurel and Abgrall [27] without heat and mass transfer in one dimension can be written as:

$$\frac{\partial \alpha_1}{\partial t} + u_I \frac{\partial \alpha_1}{\partial x} = \mu(p_1 - p_2), \tag{1a}$$

$$\frac{\partial \alpha_1 \rho_1}{\partial t} + \frac{\partial (\alpha_1 \rho_1 u_1)}{\partial x} = 0, \tag{1b}$$

$$\frac{\partial \alpha_1 \rho_1 u_1}{\partial t} + \frac{\partial (\alpha_1 \rho_1 u_1^2 + \alpha_1 p_1)}{\partial x} = p_I \frac{\partial \alpha_1}{\partial x} + \lambda(u_2 - u_1), \tag{1c}$$

$$\frac{\partial \alpha_1 \rho_1 E_1}{\partial t} + \frac{\partial (\alpha_1 (\rho_1 E_1 + p_1) u_1)}{\partial x} = p_I u_I \frac{\partial \alpha_1}{\partial x} + \mu p_I (p_2 - p_1) + \lambda u_I (u_2 - u_1), \tag{1d}$$

$$\frac{\partial \alpha_2 \rho_2}{\partial t} + \frac{\partial (\alpha_2 \rho_2 u_2)}{\partial x} = 0, \tag{1e}$$

$$\frac{\partial \alpha_2 \rho_2 u_2}{\partial t} + \frac{\partial (\alpha_2 \rho_2 u_2^2 + \alpha_2 p_2)}{\partial x} = -p_I \frac{\partial \alpha_1}{\partial x} - \lambda(u_2 - u_1), \tag{1f}$$

$$\frac{\partial \alpha_2 \rho_2 E_2}{\partial t} + \frac{\partial (\alpha_2 (\rho_2 E_2 + p_2) u_2)}{\partial x} = -p_I u_I \frac{\partial \alpha_1}{\partial x} - \mu p_I (p_2 - p_1) - \lambda u_I (u_2 - u_1). \tag{1g}$$

The notations are classical: α_k is the *volume fraction*, ρ_k the *density*, u_k the *velocity*, p_k the *pressure* and $E_k = e_k + \frac{u_k^2}{2}$ the *total specific energy*, where e_k is the *specific internal energy*.

Eq. (1a) is the evolution equation for the volume fraction of phase 1. The volume fractions for both phases are related by the saturation constraint, $\alpha_1 + \alpha_2 = 1$. The sets of Eqs. (1b)–(1d) and (1e)–(1g) express the conservation of mass, momentum and energy for phase 1 and phase 2, respectively.

The terms p_I and u_I are the *interfacial pressure* and the *interfacial velocity*, respectively. As in [27], the interfacial pressure is defined as the mixture pressure, while the interfacial velocity is defined as the velocity of the center of mass

$$p_I = \alpha_1 p_1 + \alpha_2 p_2, \quad u_I = \frac{\alpha_1 \rho_1 u_1 + \alpha_2 \rho_2 u_2}{\alpha_1 \rho_1 + \alpha_2 \rho_2}. \tag{2}$$

Other closure relations for the interfacial terms are possible. One other choice is defined by Baer and Nunziato [4] as:

$$p_I = p_1, \quad u_I = u_2.$$

Further closure relations were derived by Saurel et al. [30] and written as follows

$$\begin{aligned} p_I &= \frac{Z_1 p_2 + Z_2 p_1}{Z_1 + Z_2} + \operatorname{sign}\left(\frac{\partial \alpha_1}{\partial x}\right) \frac{(u_2 - u_1) Z_1 Z_2}{Z_1 + Z_2}, \\ u_I &= \frac{Z_1 u_1 + Z_2 u_2}{Z_1 + Z_2} + \operatorname{sign}\left(\frac{\partial \alpha_1}{\partial x}\right) \frac{p_2 - p_1}{Z_1 + Z_2}, \end{aligned} \tag{3}$$

where Z_k represents the *acoustic impedance*, $Z_k = \rho_k c_k$, where the *speed of sound* c_k is given as

$$c_k^2 = \frac{\frac{p_k}{\rho_k^2} - \left(\frac{\partial e_k}{\partial \rho_k}\right)_{p_k}}{\left(\frac{\partial e_k}{\partial p_k}\right)_{\rho_k}}, \quad k = 1, 2. \tag{4}$$

In this work for the model (1) we will use the relations that are given in (2).

The parameters λ and $\mu > 0$ that appear in the model are the relaxation parameters which determine the rates at which the velocities and pressures of the two phases relax to a common value. In this work we are interested in the instantaneous equilibrium for both the velocity and the pressure, thus the parameters λ and μ are assumed to be infinite.

The model (1) is a non strictly hyperbolic system. For details of the mathematical properties of this model see Appendix A.

2.1. Equations of state (EOS)

Equations of state are used to close the system (1). Since this model will be modified to include the heat and mass transfer, appropriate EOS are required.

Most phase transition models use a cubic EOS, like the Van der Waals EOS. But using such an EOS produces negative squared sound speed in a certain zone of the two-phase flow, the spinodal zone. This causes a loss of hyperbolicity and leads to computational failure [25,33]. To overcome this problem each fluid obeys its own EOS as a pure material, also these EOS should satisfy certain convexity constraints [19,25,33].

In this paper we will use a modified form of the stiffened gas EOS (SG-EOS) with the same parameters for the dodecane and the water as in Saurel et al. [33] and Le Métayer et al. [20]. An essential issue is that the various parameters are linked to each other to fulfill some constraints to recover the phase diagram. This makes such a choice of EOS suitable for phase transitions [20,33]. For $k = 1, 2$, they are expressed as

$$e_k(p_k, \rho_k) = \frac{p_k + \gamma_k \pi_k}{\rho_k (\gamma_k - 1)} + q_k, \tag{5a}$$

$$T_k(p_k, \rho_k) = \frac{p_k + \pi_k}{C_{vk} \rho_k (\gamma_k - 1)}, \tag{5b}$$

$$s(p_k, T_k) = C_{vk} \ln \frac{T_k^{\gamma_k}}{(p_k + \pi_k)^{(\gamma_k - 1)}} + q'_k, \tag{5c}$$

where T_k is the *temperature*, s_k the *specific entropy* and C_{vk} the *heat capacity at constant volume*. The parameters γ_k, π_k, q_k and q'_k are characteristic constants of the thermodynamic behavior of the fluid. All parameters of the SG-EOS are given in Table 1 for the water and in Table 2 for the dodecane.

Table 1
EOS parameters for vapor and liquid water.

Phase	γ	π (Pa)	C_v (J/kg/K)	C_p (J/kg/K)	q (J/kg)	q' (J/kg/K)
Vapor	1.43	0	1.04×10^3	1.487×10^3	2030×10^3	-23×10^3
Liquid	2.35	10^9	1.816×10^3	4.267×10^3	-1167×10^3	0

Table 2
EOS parameters for vapor and liquid dodecane.

Phase	γ	π (Pa)	C_v (J/kg/K)	C_p (J/kg/K)	q (J/kg)	q' (J/kg/K)
Vapor	1.025	0	1.956×10^3	2.005×10^3	-237×10^3	-24×10^3
Liquid	2.35	4×10^8	1.077×10^3	2.534×10^3	-755×10^3	0

2.2. Entropy equations

In this part we deduce the entropy equation for each phase. These equations will be used later. Denote the material derivative as

$$\frac{D_k(\cdot)}{Dt} = \frac{\partial(\cdot)}{\partial t} + u_k \frac{\partial(\cdot)}{\partial x}, \quad k = 1, 2.$$

Using the continuity Eq. (1b) with the momentum Eq. (1c), we have

$$\alpha_1 \rho_1 \frac{D_1 u_1}{Dt} + \frac{\partial \alpha_1 p_1}{\partial x} = p_I \frac{\partial \alpha_1}{\partial x} + \lambda(u_2 - u_1).$$

Multiplying this equation by u_1, we get the following equation for the *kinetic energy*

$$\alpha_1 \rho_1 \frac{D_1(\frac{u_1^2}{2})}{Dt} + u_1 \frac{\partial \alpha_1 p_1}{\partial x} = u_1 p_I \frac{\partial \alpha_1}{\partial x} + \lambda u_1(u_2 - u_1).$$

Subtracting this equation from the total energy Eq. (1d), we obtain the *internal energy equation*

$$\alpha_1 \rho_1 \frac{D_1 e_1}{Dt} + \alpha_1 p_1 \frac{\partial u_1}{\partial x} = p_I(u_I - u_1)\frac{\partial \alpha_1}{\partial x} + \mu p_I(p_2 - p_1) + \lambda(u_I - u_1)(u_2 - u_1). \tag{6}$$

From the volume fraction Eq. (1a) with the continuity Eq. (1b) we have

$$\alpha_1 \frac{D_1 \rho_1}{Dt} + \alpha_1 \rho_1 \frac{\partial u_1}{\partial x} = \rho_1(u_I - u_1)\frac{\partial \alpha_1}{\partial x} + \mu \rho_1(p_2 - p_1). \tag{7}$$

To get an equation for the entropy we use the Gibbs relation

$$T_1 ds_1 = de_1 - \frac{p_1}{\rho_1^2} d\rho_1.$$

By taking the material derivative for this relation and multiplying by $\alpha_1 \rho_1$, we obtain

$$\alpha_1 \rho_1 T_1 \frac{D_1 s_1}{Dt} = \alpha_1 \rho_1 \frac{D_1 e_1}{Dt} - \frac{\alpha_1 p_1}{\rho_1} \frac{D_1 \rho_1}{Dt}. \tag{8}$$

Using (6) and (7) in (8), we have

$$\alpha_1 \rho_1 T_1 \frac{D_1 s_1}{Dt} = (p_I - p_1)(u_I - u_1)\frac{\partial \alpha_1}{\partial x} + \mu(p_I - p_1)(p_2 - p_1) + \lambda(u_I - u_1)(u_2 - u_1).$$

In a similar way we deduce the entropy equation for phase "2" which is given as

$$\alpha_2 \rho_2 T_2 \frac{D_2 s_2}{Dt} = (p_I - p_2)(u_I - u_2)\frac{\partial \alpha_2}{\partial x} - \mu(p_I - p_2)(p_2 - p_1) - \lambda(u_I - u_2)(u_2 - u_1).$$

3. Numerical method

The source terms of the system (1) consist of differential parts and non-differential parts. As in [27] to account for both parts we use the Strang splitting approach [37]. Let $L_h^{\Delta t}$ be the operator of numerical solution of the hyperbolic part of the system (1) over Δt and $L_s^{\frac{\Delta t}{2}}$ the operator of integration of the source and relaxation terms over half of the time interval, i.e. $\frac{\Delta t}{2}$. Thus the solution is obtained by the succession of operators.

$$\mathbf{U}_j^{n+1} = L_s^{\frac{\Delta t}{2}} L_h^{\Delta t} L_s^{\frac{\Delta t}{2}} \mathbf{U}_j^n, \tag{9}$$

where $\mathbf{U} = (\alpha_1, \alpha_1\rho_1, \alpha_1\rho_1 u_1, \alpha_1\rho_1 E_1, \alpha_2\rho_2, \alpha_2\rho_2 u_2, \alpha_2\rho_2 E_2)^T$.

3.1. Hyperbolic operator

Consider the hyperbolic part of the system (1)

$$\frac{\partial \alpha_1}{\partial t} + u_I \frac{\partial \alpha_1}{\partial x} = 0, \tag{10a}$$

$$\frac{\partial \mathbf{u}}{\partial t} + \frac{\partial \mathbf{f}(\mathbf{u}, \alpha_1)}{\partial x} = \mathbf{h}(\mathbf{u}, \alpha_1)\frac{\partial \alpha_1}{\partial x}, \tag{10b}$$

where

$$\mathbf{u}=\begin{bmatrix}\alpha_1\rho_1\\ \alpha_1\rho_1u_1\\ \alpha_1\rho_1E_1\\ \alpha_2\rho_2\\ \alpha_2\rho_2u_2\\ \alpha_2\rho_2E_2\end{bmatrix},\quad \mathbf{f}(\mathbf{u},\alpha_1)=\begin{bmatrix}\alpha_1\rho_1u_1\\ \alpha_1\rho_1u_1^2+\alpha_1p_1\\ \alpha_1(\rho_1E_1+p_1)u_1\\ \alpha_2\rho_2u_2\\ \alpha_2\rho_2u_2^2+\alpha_2p_2\\ \alpha_2(\rho_2E_2+p_2)u_2\end{bmatrix},\quad \mathbf{h}(\mathbf{u},\alpha_1)=\begin{bmatrix}0\\ p_I\\ p_Iu_I\\ 0\\ -p_I\\ -p_Iu_I\end{bmatrix}.$$

Following [27] a modified Godunov scheme is used to take into account the discretization of the non-conservative part of the system (10). Assume that we have some Godunov-type discretization for the system (10b) of the form

$$\mathbf{u}_j^{n+1}=\mathbf{u}_j^n-\frac{\Delta t}{\Delta x}[\mathbf{f}(\mathbf{u}^*(\mathbf{u}_j^n,\mathbf{u}_{j+1}^n))-\mathbf{f}(\mathbf{u}^*(\mathbf{u}_{j-1}^n,\mathbf{u}_j^n))]+\Delta t\mathbf{h}_j\Delta_j, \tag{11}$$

where Δ_j is the discrete form of the term $\frac{\partial\alpha_1}{\partial x}$, which has to be determined, and $\mathbf{u}^*(\mathbf{u}_j^n,\mathbf{u}_{j+1}^n)$ is the value of $\mathbf{u}$ along the line $x=x_{j+\frac{1}{2}}$ for the Riemann problem with the states $\mathbf{u}_j^n,\mathbf{u}_{j+1}^n$.

The components of the system (11) for phase "1" can be written as

$$(\alpha\rho)_j^{n+1}=(\alpha\rho)_j^n-\frac{\Delta t}{\Delta x}\left[(\alpha\rho u)_{j+\frac{1}{2}}^*-(\alpha\rho u)_{j-\frac{1}{2}}^*\right], \tag{12a}$$

$$(\alpha\rho u)_j^{n+1}=(\alpha\rho u)_j^n-\frac{\Delta t}{\Delta x}\left[(\alpha\rho u^2+\alpha p)_{j+\frac{1}{2}}^*-(\alpha\rho u^2+\alpha p)_{j-\frac{1}{2}}^*\right]+\Delta t(p_I)_j^n\Delta_j, \tag{12b}$$

$$(\alpha\rho E)_j^{n+1}=(\alpha\rho E)_j^n-\frac{\Delta t}{\Delta x}\left[(\alpha\rho uE+\alpha pu)_{j+\frac{1}{2}}^*-(\alpha\rho uE+\alpha pu)_{j-\frac{1}{2}}^*\right]+\Delta t(p_I)_j^n(u_I)_j^n\Delta_j. \tag{12c}$$

The index "1" is omitted for simplicity.

In order to find an expression for Δ_j, the idea of Abgrall [1] is used, that a uniform pressure and velocity must remain uniform during time evolution, for more discussion about this idea see [28]. Assume p and u are a constant pressure and velocity everywhere at time t^n. Then according to the Abgrall principle we have

$$p_j^n=p_j^{n+1}=(p_I)_j^n=p_{j\pm\frac{1}{2}}^*=p, \tag{13}$$

$$u_j^n=u_j^{n+1}=(u_I)_j^n=u_{j\pm\frac{1}{2}}^*=u. \tag{14}$$

Multiplying (12a) by u and subtracting the result from (12b), we obtain

$$\Delta_j=\frac{1}{\Delta x}(\alpha_{j+\frac{1}{2}}^*-\alpha_{j-\frac{1}{2}}^*). \tag{15}$$

Using the definition of E and (15) in (12c), and using (12a), we have the following equation for internal energy

$$(\alpha\rho e)_j^{n+1}=(\alpha\rho e)_j^n-\frac{\Delta t}{\Delta x}u\left[(\alpha\rho e)_{j+\frac{1}{2}}^*-(\alpha\rho e)_{j-\frac{1}{2}}^*\right]. \tag{16}$$

Multiplying (12a) by the parameter q in the (5a) and subtracting the result from (16), we obtain

$$(\alpha\rho(e-q))_j^{n+1}=(\alpha\rho(e-q))_j^n-\frac{\Delta t}{\Delta x}u\left[(\alpha\rho(e-q))_{j+\frac{1}{2}}^*-(\alpha\rho(e-q))_{j-\frac{1}{2}}^*\right]. \tag{17}$$

From the EOS (5a) and uniformity of pressure (13), we see that

$$\rho(e-q)=\frac{p+\gamma\pi}{\gamma-1}=const. \tag{18}$$

Thus from (17) with (18), we get by taking out the constant and using (14)

$$\alpha_j^{n+1}=\alpha_j^n-(u_I)_j^n\frac{\Delta t}{\Delta x}\left(\alpha_{j+\frac{1}{2}}^*-\alpha_{j-\frac{1}{2}}^*\right). \tag{19}$$

This equation provides a discretization for the volume fraction equation.

For the Riemann values the approximate solvers HLL, HLLC [38] and VFRoe [12] are used. For the seven-equation model (1) the HLL solver is introduced in [27] and the VFRoe solver is considered in [3]. In the following section we present the HLLC solver.

3.1.1. HLLC-type solver

The intercell flux of the HLLC Riemann solver is given by, see Toro [38]

$$\mathbf{F}^{HLLC}_{j+\frac{1}{2}} = \begin{cases} \mathbf{f}(\mathbf{u}_L), & 0 \leqslant s_L, \\ \mathbf{f}(\mathbf{u}_{*L}) = \mathbf{f}(\mathbf{u}_L) + s_L(\mathbf{u}_{*L} - \mathbf{u}_L), & s_L \leqslant 0 \leqslant s_*, \\ \mathbf{f}(\mathbf{u}_{*R}) = \mathbf{f}(\mathbf{u}_R) + s_R(\mathbf{u}_{*R} - \mathbf{u}_R), & s_* \leqslant 0 \leqslant s_R, \\ \mathbf{f}(\mathbf{u}_R), & 0 \geqslant s_R. \end{cases}$$

where 'L' and 'R' refer to the left and right states of a cell boundary respectively.

Following the Davis estimates [8] the wave speeds can be taken as

$$s_L = \min\{u_{1L} - c_{1L}, u_{2L} - c_{2L}, u_{1R} - c_{1R}, u_{2R} - c_{2R}\},$$
$$s_R = \max\{u_{1L} + c_{1L}, u_{2L} + c_{2L}, u_{1R} + c_{1R}, u_{2R} + c_{2R}\}.$$

Following Toro [38] for a single phase, the vectors $\mathbf{u}_{*L}$ and $\mathbf{u}_{*R}$ can be given as

$$\mathbf{u}_{*K} = \begin{bmatrix} \alpha_{1K}\rho_{1K}\frac{s_K - u_{1K}}{s_K - s_*} \\ \alpha_{1K}\rho_{1K}\frac{s_K - u_{1K}}{s_K - s_*}s_* \\ \alpha_{1K}\rho_{1K}\frac{s_K - u_{1K}}{s_K - s_*}\left(E_{1K} + (s_* - u_{1K})\left(s_* + \frac{p_{1K}}{\rho_{1K}(s_K - u_{1K})}\right)\right) \\ \alpha_{2K}\rho_{2K}\frac{s_K - u_{2K}}{s_K - s_*} \\ \alpha_{2K}\rho_{2K}\frac{s_K - u_{2K}}{s_K - s_*}s_* \\ \alpha_{2K}\rho_{2K}\frac{s_K - u_{2K}}{s_K - s_*}\left(E_{2K} + (s_* - u_{2K})\left(s_* + \frac{p_{2K}}{\rho_{2K}(s_K - u_{2K})}\right)\right) \end{bmatrix}, \quad K = L, R.$$

We take the speed s_* as in [38] but with mixture values for pressure, velocity and density, i.e.

$$s_* = \frac{p_R - p_L + \rho_L u_L(s_L - u_L) - \rho_R u_R(s_R - u_R)}{\rho_L(s_L - u_L) - \rho_R(s_R - u_R)}$$

where $\rho = \alpha_1\rho_1 + \alpha_2\rho_2, p = \alpha_1 p_1 + \alpha_2 p_2$ and $u = \frac{\alpha_1\rho_1 u_1 + \alpha_2\rho_2 u_2}{\rho}$.

We refer to the mathematical properties of the model (1) in Appendix A. Consider the eigenvectors (A.4) and (A.5) for the 2- to 7-fields. It is clear that the function $\varphi(\mathbf{W}) = \alpha_1$ is a Riemann invariant for all 2- to 7-characteristic fields. This means that α_1 is constant across all rarefaction waves of the 2- to 7-fields. Also note that the action of the non-conservative terms is reflected in the 1-field which corresponds to the eigenvalue $\lambda_1 = u_I$. Moreover, this eigenvalue comes from the evolutionary equation for α_1. Considering these observations we will assume that α_1 changes only across s_*, this means that

$$\alpha_{1*K} = \alpha_{1K}, \quad K = L, R.$$

3.1.2. Extension to the second-order

To achieve second-order accuracy we use the MUSCL method, where MUSCL stands for Monotone Upstream-centered Scheme for Conservation Laws. In the following we will give a summary of this method, and for details we refer to Toro [38]. This method has three steps, they are

- *Data reconstruction:* The primitive variables on the cell boundary are extrapolated as

$$\mathbf{W}^-_{j+\frac{1}{2}} = \mathbf{W}^n_j + \frac{1}{2}\delta_j, \quad \mathbf{W}^+_{j-\frac{1}{2}} = \mathbf{W}^n_j - \frac{1}{2}\delta_j.$$

Performing this step in primitive variables ensures the preservation of uniformity of pressure and velocity, which is an essential issue in the discretization of the model.

The limited slope δ_j is taken as

$$\delta_j = \begin{cases} \max\left\{0, \min(\beta d_{j-\frac{1}{2}}, d_{j+\frac{1}{2}}), \min(d_{j-\frac{1}{2}}, \beta d_{j+\frac{1}{2}})\right\}, & d_{j+\frac{1}{2}} > 0 \\ \min\left\{0, \max(\beta d_{j-\frac{1}{2}}, d_{j+\frac{1}{2}}), \max(d_{j-\frac{1}{2}}, \beta d_{j+\frac{1}{2}})\right\}, & d_{j+\frac{1}{2}} < 0 \end{cases}$$

where

$$d_{j-\frac{1}{2}} = \mathbf{W}^n_j - \mathbf{W}^n_{j-1}, \quad d_{j+\frac{1}{2}} = \mathbf{W}^n_{j+1} - \mathbf{W}^n_j.$$

For particular values of β, the value $\beta = 1$ corresponds to the minmod limiter and $\beta = 2$ corresponds to the superbee limiter.

- *Evolution*: Using (A.1) the values $\mathbf{W}^{\pm}_{j\mp\frac{1}{2}}$ are evolved by a time $\frac{\Delta t}{2}$ as

$$\widehat{\mathbf{W}}^{+}_{j-\frac{1}{2}} = \mathbf{W}^{+}_{j-\frac{1}{2}} - \frac{\Delta t}{2\Delta x}\mathbf{A}(\mathbf{W}_j)(\mathbf{W}^{-}_{j+\frac{1}{2}} - \mathbf{W}^{+}_{j-\frac{1}{2}}),$$
$$\widehat{\mathbf{W}}^{-}_{j+\frac{1}{2}} = \mathbf{W}^{-}_{j+\frac{1}{2}} - \frac{\Delta t}{2\Delta x}\mathbf{A}(\mathbf{W}_j)(\mathbf{W}^{-}_{j+\frac{1}{2}} - \mathbf{W}^{+}_{j-\frac{1}{2}}).$$

- *Solution of the Riemann problem:* We rewrite $\widehat{\mathbf{W}}^{\pm}_{j\pm\frac{1}{2}}$ in conservative form, and solve the Riemann problem with the piecewise constant data $(\widehat{\mathbf{U}}^{-}_{j+\frac{1}{2}}, \widehat{\mathbf{U}}^{+}_{j+\frac{1}{2}})$.

3.2. Source and relaxation operators

According to the Strang splitting (9), to take into account for source and relaxation terms we have to solve the following system of ordinary differential equations (ODE).

$$\frac{d\mathbf{U}}{dt} = \mathbf{S} \tag{20}$$

where $\mathbf{U} = (\alpha_1, \alpha_1\rho_1, \alpha_1\rho_1 u_1, \alpha_1\rho_1 E_1, \alpha_2\rho_2, \alpha_2\rho_2 u_2, \alpha_2\rho_2 E_2)^T$. The source vector $\mathbf{S}$ can be decomposed as the sum

$$\mathbf{S} = \mathbf{S}_V + \mathbf{S}_P + \mathbf{S}_{Thermal},$$

where $\mathbf{S}_V$ and $\mathbf{S}_P$ are associated with velocity and pressure relaxation terms respectively. The vector $\mathbf{S}_{Thermal}$ represents the thermal relaxation terms that include the temperature and Gibbs free energy relaxation terms that have to be modeled. The mechanical relaxation terms $\mathbf{S}_V$ and $\mathbf{S}_P$ are given by

$$\mathbf{S}_V = \begin{bmatrix} 0 \\ 0 \\ \lambda(u_2-u_1) \\ \lambda u_I(u_2-u_1) \\ 0 \\ -\lambda(u_2-u_1) \\ -\lambda u_I(u_2-u_1) \end{bmatrix}, \quad \text{and } \mathbf{S}_P = \begin{bmatrix} \mu(p_1-p_2) \\ 0 \\ 0 \\ \mu p_I(p_2-p_1) \\ 0 \\ 0 \\ -\mu p_I(p_2-p_1) \end{bmatrix}.$$

The system (20) is solved by successive integrations considering each one of the source vectors alone.

The relaxation time scales depend on many parameters of the fluids and also possibly on the process, i.e. evaporation, condensation, combustion, etc. For example the rate of the pressure relaxation μ depends on the compressibility of each fluid besides the nature of each fluid and the two-phase mixture topology [27,31]. The velocity relaxation time may be greater than that required for the pressure relaxation, since the velocity relaxation depends on the fluid viscosity which has slow effects compared to others, also it depends on the pressure relaxation which is in general fast compared to the longitudinal wave propagation [27,31]. The interface conditions, for the interface that separates two pure fluids, impose an equality for pressure and velocity. In many physical situations it is reasonable to assume that the pressure and velocity relax instantaneously. Such an assumption also fulfills the interface conditions. Some estimations in certain situations show that the time scale of the velocity relaxation and pressure relaxation are of the same order of magnitude [7,26].

The temperature relaxation depends on the thermal conductivity of the fluids. Where this conduction occurs due to the collisions of the molecules of the fluids. To reach temperature equilibrium a large number of collisions is required. This in general has long characteristic time compared to the pressure and velocity relaxation.

The Gibbs free energy relaxation parameter depends on local chemical relaxation [33]. And this is a slow process compared with other processes that related to the pressure, velocity and temperature relaxation at the interfaces. Therefore the relaxation time of the Gibbs free energy relaxation is the longest compared to other relaxation times.

In this paper we assume that the relaxation times are very close to zero i.e. instantaneous relaxations. This assumption is justified for the pressure and the velocity in the entire flow field. For the temperature and the Gibbs free energy this assumption is considered only at the interface where the heat and mass transfer occur, indeed this assumption is standard at equilibrium interfaces when mass transfer occurs [33]. The assumption of instantaneous relaxations means that all relaxation parameters are taken to be infinite and this makes the model free of parameters.

Moreover we assume that the relaxation time of the mechanical variables is much smaller than that of the thermal variables. We assume that the mechanical variables relax very fast to equilibrium values, and they will stay in equilibrium during the thermal relaxation. Also we assume that the temperature relaxes much faster than the Gibbs free energy.

For the velocity and pressure relaxation we use the same procedures as Saurel and Abgrall [27], other procedures for pressure relaxation also are possible, see [17,18,31]. For the thermal relaxation terms we modeled them depending on the observation of the differences between relaxation times for various variables, they are the subject of the next section.

4. Thermal relaxation, modeling of heat and mass transfer

At each time step after the procedures for the velocity and pressure relaxations we have a two-phase mixture in mechanical equilibrium, but each phase has its own temperature and its own Gibbs free energy. In this section we will insert the effect of heat and mass transfer that take place at the interface.

To locate the interface we use the ideas of Saurel et al. [33], that the cell is filled with pure fluid when its volume fraction is close to 1, say $(1-\epsilon)$, with $\epsilon = 10^{-6}$. The interface corresponds to mixture cells when the volume fraction ranges between $\bar{\epsilon}$ and $1-\bar{\epsilon}$, with $\bar{\epsilon} = 10^{-4}$. The value of $\bar{\epsilon}$ has to be chosen larger than the value of ϵ to ensure that phase transitions occur only in the interfacial zone, for a discussion on this point see [33]. Also mass transfer is allowed if the liquid is metastable, i.e. $T_l > T_{sat}(p_{equi})$. For the computation of the curve $T = T_{sat}(p_{equi})$ see Appendix C.

According to our assumption that the mechanical relaxation time is very small compared with the thermal relaxation time we may also assume that the mechanical quantities will stay in equilibrium during the thermal relaxation. Therefore, our modeled terms will keep this assumption.

Also we assume that the temperature relaxes much faster than the Gibbs free energy. So we will split the thermal terms into two parts. One is related to the heat transfer $\mathbf{S}_Q$ and the other is related to the mass transfer $\mathbf{S}_m$, i.e.

$$\mathbf{S}_{Thermal} = \mathbf{S}_Q + \mathbf{S}_m.$$

The system of ODE (20) is solved for the temperature relaxation then for the Gibbs free energy relaxation. During the Gibbs free energy relaxation we assume that the temperature will stay in equilibrium, and our modeled terms will keep this condition.

4.1. Heat transfer and temperature relaxation

The heat transfer is added through the temperature relaxation terms. In the model (1) the heat transfer term Q initially appears in the energy equations. As the pressure equilibrium is maintained through the temperature relaxation we will modify the volume fraction equation to include the effect of the heat transfer in a way to be able to keep an equilibrium pressure during the temperature relaxation process. Therefore the heat source vector $\mathbf{S}_Q$ is modeled as

$$\mathbf{S}_Q = \left(\frac{Q}{\kappa}, 0, 0, Q, 0, 0, -Q\right)^T, \tag{21}$$

where the new variable κ has to be determined.

Then to take into account for the heat transfer we have to solve the following system of ODE

$$\frac{d\mathbf{U}}{dt} = \mathbf{S}_Q. \tag{22}$$

To find the expression for κ we will use the assumption that the pressure will stay in equilibrium, and to do that we assume

$$\frac{\partial p_1}{\partial t} = \frac{\partial p_2}{\partial t}. \tag{23}$$

4.1.1. Determination of κ

Consider the components of the system (22) for phase "1"

$$\frac{\partial \alpha_1}{\partial t} = \frac{Q}{\kappa}, \tag{24a}$$

$$\frac{\partial \alpha_1 \rho_1}{\partial t} = 0, \tag{24b}$$

$$\frac{\partial \alpha_1 \rho_1 u_1}{\partial t} = 0, \tag{24c}$$

$$\frac{\partial \alpha_1 \rho_1 E_1}{\partial t} = Q. \tag{24d}$$

From (24a) and (24d) we obtain

$$\frac{\partial \alpha_1 \rho_1 E_1}{\partial t} = \kappa \frac{\partial \alpha_1}{\partial t}. \tag{25}$$

Using the definition of E_1, (24b) and (24c) with (25) we have

$$\alpha_1 \rho_1 \frac{\partial e_1}{\partial t} = \kappa \frac{\partial \alpha_1}{\partial t}. \tag{26}$$

The internal energy e_1 is expressed in terms of p_1 and ρ_1, i.e. $e_1 = e_1(p_1, \rho_1)$. Differentiating it with respect to t and substituting the result in (26), we obtain

$$\alpha_1\rho_1\left(\frac{\partial e_1}{\partial p_1}\right)_{\rho_1}\frac{\partial p_1}{\partial t} + \alpha_1\rho_1\left(\frac{\partial e_1}{\partial \rho_1}\right)_{p_1}\frac{\partial \rho_1}{\partial t} = \kappa\frac{\partial \alpha_1}{\partial t}. \tag{27}$$

From (24b) we have $\alpha_1\frac{\partial \rho_1}{\partial t} = -\rho_1\frac{\partial \alpha_1}{\partial t}$. Using this in (27) we get

$$\alpha_1\rho_1\left(\frac{\partial e_1}{\partial p_1}\right)_{\rho_1}\frac{\partial p_1}{\partial t} - \rho_1^2\left(\frac{\partial e_1}{\partial \rho_1}\right)_{p_1}\frac{\partial \alpha_1}{\partial t} = \kappa\frac{\partial \alpha_1}{\partial t},$$

or

$$\frac{\partial p_1}{\partial t} = \frac{\kappa + \rho_1^2\left(\frac{\partial e_1}{\partial \rho_1}\right)_{p_1}}{\alpha_1\rho_1\left(\frac{\partial e_1}{\partial p_1}\right)_{\rho_1}}\frac{\partial \alpha_1}{\partial t}. \tag{28}$$

A similar equation can be attained for p_2

$$\frac{\partial p_2}{\partial t} = -\frac{\kappa + \rho_2^2\left(\frac{\partial e_2}{\partial \rho_2}\right)_{p_2}}{\alpha_2\rho_2\left(\frac{\partial e_2}{\partial p_2}\right)_{\rho_2}}\frac{\partial \alpha_1}{\partial t}. \tag{29}$$

Using (28) and (29) in the condition (23) and after some manipulations we have the following expression for κ

$$\kappa = \frac{\frac{\rho_1 c_1^2}{\alpha_1} + \frac{\rho_2 c_2^2}{\alpha_2}}{\frac{\Gamma_1}{\alpha_1} + \frac{\Gamma_2}{\alpha_2}} - \frac{\frac{\Gamma_1}{\alpha_1}p_1 + \frac{\Gamma_2}{\alpha_2}p_2}{\frac{\Gamma_1}{\alpha_1} + \frac{\Gamma_2}{\alpha_2}}. \tag{30}$$

Here Γ_k denotes the Grüneisen coefficient of phase k which is given as

$$\Gamma_k = \frac{1}{\rho_k}\left(\frac{\partial p_k}{\partial e_k}\right)_{\rho_k}, \quad k = 1, 2. \tag{31}$$

Since the heat transfer relaxation is considered when pressure equilibrium is maintained, i.e. $p_1 = p_2 = p_{eq}$, the second term in the right hand side of (30) is equivalent to the equilibrium pressure. Thus we have

$$\kappa = \frac{\frac{\rho_1 c_1^2}{\alpha_1} + \frac{\rho_2 c_2^2}{\alpha_2}}{\frac{\Gamma_1}{\alpha_1} + \frac{\Gamma_2}{\alpha_2}} - p_{eq}. \tag{32}$$

It is interesting to note that the first term on the right hand side of (32) is exactly the same term that appears in a similar manner with heat transfer that is given in the model of Saurel et al. [33].

In the context of the SG-EOS (5), we have the following expression for κ

$$\kappa = \frac{\frac{p_1+\gamma_1\pi_1}{\alpha_1} + \frac{p_2+\gamma_2\pi_2}{\alpha_2}}{\frac{\gamma_1-1}{\alpha_1} + \frac{\gamma_2-1}{\alpha_2}}.$$

4.1.2. Mixture entropy

Now let us consider the equation of the mixture entropy. If we follow the same method in Section 2.2 for the model with new modifications, we have

$$\alpha_1\rho_1 T_1\frac{Ds_1}{Dt} = (1 + \frac{p_1}{\kappa})Q, \tag{33a}$$

$$\alpha_2\rho_2 T_2\frac{Ds_2}{Dt} = -(1 + \frac{p_2}{\kappa})Q. \tag{33b}$$

After the mechanical relaxation p_1 and p_2 are in equilibrium, so $p_1 = p_2 = p_{eq}$.

Combining the two equations in (33) we get the following equation for the mixture entropy

$$\frac{\partial \rho s}{\partial t} + \frac{\partial \rho s u}{\partial x} = (1 + \frac{p_{eq}}{\kappa})Q\left(\frac{T_2 - T_1}{T_1 T_2}\right),$$

where $\rho s = \alpha_1\rho_1 s_1 + \alpha_2\rho_2 s_2$ and $u = u_1 = u_2$ is the equilibrium velocity.

The heat transfer Q is modeled as $Q = \theta(T_2 - T_1)$, where $\theta > 0$ is the temperature relaxation parameter. Since κ is always positive the mixture entropy satisfies the second law of thermodynamics, i.e.

$$\frac{\partial \rho s}{\partial t} + \frac{\partial \rho s u}{\partial x} = \theta\left(1 + \frac{p_{eq}}{\kappa}\right)\frac{(T_2 - T_1)^2}{T_1 T_2} \geqslant 0.$$

In this work the parameter θ is assumed to tend to infinity, i.e. the temperature relaxes to a common value instantaneously at any time. This assumption is considered at the interface only.

4.1.3. Temperature relaxation

Now to solve the system (24) with $\theta \to \infty$, we proceed as for the pressure relaxation in [27]. It is clear that $\alpha_1\rho_1$ and $\alpha_1\rho_1 u_1$, therefore also u_1 stay constant through the relaxation process.

From the system (24) we obtain (26) for the internal energy, which can be rewritten as

$$\frac{\partial e_1}{\partial t} = \frac{\kappa}{\alpha_1\rho_1}\frac{\partial \alpha_1}{\partial t}.$$

Integrating this equation, we obtain the following approximation

$$e_1^* = e_1^0 + \frac{\bar{\kappa}}{\alpha_1^0\rho_1^0}(\alpha_1^* - \alpha_1^0) \tag{34}$$

where '0' and '*' refer to the states before and after the relaxation process respectively and $\bar{\kappa}$ is the mean interfacial value between the states $(\alpha_1^0, \rho_1^0, e_1^0)$ and $(\alpha_1^*, \rho_1^*, e_1^*)$. Also, we can proceed in the same way to get a similar result for phase '2'.

We consider (34) as an equation for e_1 as a function of α_1, i.e. $e_1 = e_1^0 + \frac{\bar{\kappa}}{\alpha_1^0\rho_1^0}(\alpha_1 - \alpha_1^0)$, and from (24b) $\rho_1 = \frac{const}{\alpha_1}$. And analogously for the other phase, since $\alpha_2 = 1 - \alpha_1$ we have only one variable α_1 in the relation

$$f_T(\alpha_1) = T_2(e_2, \rho_2) - T_1(e_1, \rho_1) = 0. \tag{35}$$

Our aim now is to find an α_1 that satisfies the equilibrium condition (35). The variable $\bar{\kappa}$ can be approximated as $\bar{\kappa} = \frac{\tilde{\kappa}+\kappa^0}{2}$, where $\tilde{\kappa}$ is estimated at the new state resulting from iterative procedure for solving $f_T(\alpha_1) = 0$.

In this way we get the temperature equilibrium, while keeping the mechanical equilibrium.

4.2. Mass transfer and Gibbs free energy relaxation

Analogous to the heat transfer, the mass transfer is also modeled through relaxation terms. As mentioned we assume that the temperature relaxation time is very small compared with the Gibbs free energy relaxation time, and so we will consider that the mechanical equilibrium and the equilibrium of temperature will be satisfied through the Gibbs free energy relaxation.

To take into account the mass transfer we have to solve the following system of ODE

$$\frac{d\mathbf{U}}{dt} = \mathbf{S}_m. \tag{36}$$

Our aim now is to model the mass transfer source vector $\mathbf{S}_m$. The literature on averaging techniques shows that the mass transfer appears in the model as a mass rate in the interfacial momentum and in the interfacial energy, see [9,10,14]. But the expressions for these terms are unknown. Here we will insert these terms in the model as they appear by averaging, but we will use some assumptions to find certain expressions for these terms.

Let us assume that $\mathbf{S}_m$ is given in the model as

$$\frac{\partial \alpha_1}{\partial t} = \frac{\dot{m}}{\varrho}, \tag{37a}$$

$$\frac{\partial \alpha_1\rho_1}{\partial t} = \dot{m}, \tag{37b}$$

$$\frac{\partial \alpha_1\rho_1 u_1}{\partial t} = u_I\dot{m}, \tag{37c}$$

$$\frac{\partial \alpha_1\rho_1 E_1}{\partial t} = \left(e_i + \frac{u_I^2}{2}\right)\dot{m}, \tag{37d}$$

$$\frac{\partial \alpha_2\rho_2}{\partial t} = -\dot{m}, \tag{37e}$$

$$\frac{\partial \alpha_2\rho_2 u_2}{\partial t} = -u_I\dot{m}, \tag{37f}$$

$$\frac{\partial \alpha_2\rho_2 E_2}{\partial t} = -\left(e_i + \frac{u_I^2}{2}\right)\dot{m}. \tag{37g}$$

The new variables ϱ and e_i have to be determined. According to our assumption the relaxation time of the Gibbs free energy is much larger than other relaxation times, so during the Gibbs free energy relaxation process we will assume that the pressure and temperature stay in equilibrium. Thus to find the new variables we use the following assumptions

$$\frac{\partial p_1}{\partial t} = \frac{\partial p_2}{\partial t}, \tag{38a}$$

$$\frac{\partial T_1}{\partial t} = \frac{\partial T_2}{\partial t}. \tag{38b}$$

4.2.1. Determination of e_i and ϱ

Since the model (37) is solved after the mechanical relaxation we have $u_1 = u_2 = u_I$. From (37b) and (37c) the velocity u_1 is constant through the relaxation procedure, also from (37e) and (37f) the velocity u_2 is constant.

Using the Eqs. (37a)–(37d) and the definition of E_1, we get

$$\alpha_1\rho_1\frac{\partial e_1}{\partial t} = (e_i - e_1)\dot{m}. \tag{39}$$

Differentiate $e_1(p_1, \rho_1)$ with respect to t and substitute the result in (39). We obtain

$$\alpha_1\rho_1\left(\frac{\partial e_1}{\partial p_1}\right)_{\rho_1}\frac{\partial p_1}{\partial t} + \alpha_1\rho_1\left(\frac{\partial e_1}{\partial \rho_1}\right)_{p_1}\frac{\partial \rho_1}{\partial t} = \varrho(e_i - e_1)\frac{\partial \alpha_1}{\partial t}. \tag{40}$$

From (37a) and (37b), we get

$$\alpha_1\frac{\partial \rho_1}{\partial t} = (\varrho - \rho_1)\frac{\partial \alpha_1}{\partial t}. \tag{41}$$

Using this in (40), we have

$$\alpha_1\rho_1\left(\frac{\partial e_1}{\partial p_1}\right)_{\rho_1}\frac{\partial p_1}{\partial t} + \rho_1(\varrho - \rho_1)\left(\frac{\partial e_1}{\partial \rho_1}\right)_{p_1}\frac{\partial \alpha_1}{\partial t} = \varrho(e_i - e_1)\frac{\partial \alpha_1}{\partial t}. \tag{42}$$

This leads to

$$\frac{\partial p_1}{\partial t} = \frac{\Gamma_1}{\alpha_1}\left(-\rho_1(\varrho - \rho_1)\left(\frac{\partial e_1}{\partial \rho_1}\right)_{p_1} + \varrho(e_i - e_1)\right)\frac{\partial \alpha_1}{\partial t}. \tag{43}$$

In a similar way we have an equation for p_2

$$\frac{\partial p_2}{\partial t} = -\frac{\Gamma_2}{\alpha_2}\left(-\rho_2(\varrho - \rho_2)\left(\frac{\partial e_2}{\partial \rho_2}\right)_{p_2} + \varrho(e_i - e_2)\right)\frac{\partial \alpha_1}{\partial t}. \tag{44}$$

By the condition (38a) with (43) and (44), we obtain

$$\frac{\Gamma_1}{\alpha_1}\left(-\rho_1(\varrho - \rho_1)\left(\frac{\partial e_1}{\partial \rho_1}\right)_{p_1} + \varrho(e_i - e_1)\right) = -\frac{\Gamma_2}{\alpha_2}\left(-\rho_2(\varrho - \rho_2)\left(\frac{\partial e_2}{\partial \rho_2}\right)_{p_2} + \varrho(e_i - e_2)\right). \tag{45}$$

On the other hand, e_1 can be written in terms of T_1 and ρ_1, i.e. $e_1 = e_1(T_1, \rho_1)$. Differentiating it with respect to t, substituting the result in (39) and using (41), we get

$$\frac{\partial T_1}{\partial t} = \frac{1}{\alpha_1\rho_1\left(\frac{\partial e_1}{\partial T_1}\right)_{\rho_1}}\left(-\rho_1(\varrho - \rho_1)\left(\frac{\partial e_1}{\partial \rho_1}\right)_{T_1} + \varrho(e_i - e_1)\right)\frac{\partial \alpha_1}{\partial t}.$$

But $\left(\frac{\partial e_1}{\partial T_1}\right)_{\rho_1} = C_{v1}$, the specific heat at constant volume. Thus

$$\frac{\partial T_1}{\partial t} = \frac{1}{\alpha_1\rho_1 C_{v1}}\left(-\rho_1(\varrho - \rho_1)\left(\frac{\partial e_1}{\partial \rho_1}\right)_{T_1} + \varrho(e_i - e_1)\right)\frac{\partial \alpha_1}{\partial t}. \tag{46}$$

A similar equation can be attained for T_2

$$\frac{\partial T_2}{\partial t} = \frac{-1}{\alpha_2\rho_2 C_{v2}}\left(-\rho_2(\varrho - \rho_2)\left(\frac{\partial e_2}{\partial \rho_2}\right)_{T_2} + \varrho(e_i - e_2)\right)\frac{\partial \alpha_1}{\partial t}. \tag{47}$$

By the condition (38b) with (46) and (47), we get

$$\frac{1}{\alpha_1\rho_1 C_{v1}}\left(-\rho_1(\varrho - \rho_1)\left(\frac{\partial e_1}{\partial \rho_1}\right)_{T_1} + \varrho(e_i - e_1)\right) = \frac{-1}{\alpha_2\rho_2 C_{v2}}\left(-\rho_2(\varrho - \rho_2)\left(\frac{\partial e_2}{\partial \rho_2}\right)_{T_2} + \varrho(e_i - e_2)\right). \tag{48}$$

It is clear now that (45) and (48) are two equations for the two unknowns e_i and ϱ. After some manipulations, we get from these equations

$$\varrho = \frac{\phi\left(\frac{\rho_1 c_1^2}{\alpha_1} + \frac{\rho_2 c_2^2}{\alpha_2}\right) - \phi\left(\frac{\Gamma_1}{\alpha_1} p_1 + \frac{\Gamma_2}{\alpha_2} p_2\right) + \psi\left(\frac{\rho_1^2 \left(\frac{\partial e_1}{\partial \rho_1}\right)_{T_1}}{\alpha_1 \rho_1 C_{v1}} + \frac{\rho_2^2 \left(\frac{\partial e_2}{\partial \rho_2}\right)_{T_2}}{\alpha_2 \rho_2 C_{v2}}\right)}{\phi\left(\frac{c_1^2}{\alpha_1} + \frac{c_2^2}{\alpha_2}\right) - \phi\left(\frac{\Gamma_1}{\alpha_1} h_1 + \frac{\Gamma_2}{\alpha_2} h_2\right) + \psi\left(\frac{e_1 + \rho_1 \left(\frac{\partial e_1}{\partial \rho_1}\right)_{T_1}}{\alpha_1 \rho_1 C_{v1}} + \frac{e_2 + \rho_2 \left(\frac{\partial e_2}{\partial \rho_2}\right)_{T_2}}{\alpha_2 \rho_2 C_{v2}}\right)}, \tag{49a}$$

$$e_i = \frac{\frac{e_1 + \rho_1 \left(\frac{\partial e_1}{\partial \rho_1}\right)_{T_1}}{\alpha_1 \rho_1 C_{v1}} + \frac{e_2 + \rho_2 \left(\frac{\partial e_2}{\partial \rho_2}\right)_{T_2}}{\alpha_2 \rho_2 C_{v2}}}{\phi} - \frac{\frac{\rho_1^2 \left(\frac{\partial e_1}{\partial \rho_1}\right)_{T_1}}{\alpha_1 \rho_1 C_{v1}} + \frac{\rho_2^2 \left(\frac{\partial e_2}{\partial \rho_2}\right)_{T_2}}{\alpha_2 \rho_2 C_{v2}}}{\varrho \phi} \tag{49b}$$

where $\phi = \frac{1}{\alpha_1 \rho_1 C_{v1}} + \frac{1}{\alpha_2 \rho_2 C_{v2}}, \psi = \frac{\Gamma_1}{\alpha_1} + \frac{\Gamma_2}{\alpha_2}$ and $h_k = e_k + \frac{p_k}{\rho_k}$ is the *enthalpy* for phase k.

Consider the expression of ϱ given by (49a), the terms that are multiplied by ψ come from the temperature equilibrium condition. While the terms that are multiplied by ϕ come from the pressure equilibrium condition. It is interesting to see that a similar expression is given in the Saurel et al. [33] by $\rho_I = (\frac{\rho_1 c_1^2}{\alpha_1} + \frac{\rho_2 c_2^2}{\alpha_2})/(\frac{c_1^2}{\alpha_1} + \frac{c_2^2}{\alpha_2})$, see relation (5.9) in [33]. The term ρ_I in [33] appears with the volume fraction equation in the same way as our variable ϱ, see volume fraction Eq. (37a). It is obvious that all terms of ρ_I appear in the expression of ϱ. Note also that the terms are related to the equilibrium of the temperature in the variable ϱ do not appear in the variable ρ_I, this is due to the fact that ρ_I uses the pressure equilibrium with other assumptions, but it does not use the temperature equilibrium condition.

In the context of the SG-EOS we have the following expressions for ϱ and e_i,

$$\varrho = \frac{\phi\left(\frac{p_1 + \gamma_1 \pi_1}{\alpha_1} + \frac{p_2 + \gamma_2 \pi_2}{\alpha_2}\right) - \psi\left(\frac{\pi_1}{\alpha_1 \rho_1 C_{v1}} + \frac{\pi_2}{\alpha_2 \rho_2 C_{v2}}\right)}{-\phi\left(\frac{(\gamma_1 - 1) q_1}{\alpha_1} + \frac{(\gamma_2 - 1) q_2}{\alpha_2}\right) + \psi\left(\frac{e_1 - \frac{\pi_1}{\rho_1}}{\alpha_1 \rho_1 C_{v1}} + \frac{e_2 - \frac{\pi_2}{\rho_2}}{\alpha_2 \rho_2 C_{v2}}\right)},$$

$$e_i = \frac{\left(\frac{e_1 - \frac{\pi_1}{\rho_1}}{\alpha_1 \rho_1 C_{v1}} + \frac{e_2 - \frac{\pi_2}{\rho_2}}{\alpha_2 \rho_2 C_{v2}}\right)}{\phi} + \frac{\left(\frac{\pi_1}{\alpha_1 \rho_1 C_{v1}} + \frac{\pi_2}{\alpha_2 \rho_2 C_{v2}}\right)}{\varrho \phi}.$$

Note that $\Gamma_k = \gamma_k - 1, k = 1, 2$, for the SG-EOS.

4.2.2. Mixture entropy

Now we consider the equation of mixture entropy. If we follow the same argument as in Section 2.2, under the mechanical equilibrium and temperature equilibrium, we have

$$\alpha_1 \rho_1 T_1 \frac{Ds_1}{Dt} = (e_i + \frac{p_1}{\varrho})\dot{m} - (e_1 + \frac{p_{eq}}{\rho_1})\dot{m}, \tag{51a}$$

$$\alpha_2 \rho_2 T_2 \frac{Ds_2}{Dt} = -(e_i + \frac{p_2}{\varrho})\dot{m} + (e_2 + \frac{p_{eq}}{\rho_2})\dot{m}. \tag{51b}$$

Using the mass Eqs. (37b) and (37e) with system (51), we have

$$T_1(\frac{\partial \alpha_1 \rho_1 s_1}{\partial t} + \frac{\partial \alpha_1 \rho_1 s_1 u_1}{\partial x}) = (e_i + \frac{p_{eq}}{\varrho})\dot{m} - (e_1 + \frac{p_1}{\rho_1} - T_1 s_1)\dot{m}, \tag{52a}$$

$$T_2(\frac{\partial \alpha_2 \rho_2 s_2}{\partial t} + \frac{\partial \alpha_2 \rho_2 s_2 u_2}{\partial x}) = -(e_i + \frac{p_{eq}}{\varrho})\dot{m} + (e_2 + \frac{p_2}{\rho_2} - T_2 s_2)\dot{m}. \tag{52b}$$

Note that the quantity $e_k + \frac{p_k}{\rho_k} - T_k s_k$, $k = 1, 2$ is the Gibbs free energy. Let us denote g_k for the Gibbs free energy.

Add the two entropy equations in (52) after division by temperatures, we obtain

$$\frac{\partial \rho s}{\partial t} + \frac{\partial \rho s u}{\partial x} = (e_i + \frac{p_{eq}}{\varrho})\dot{m}\left(\frac{T_2 - T_1}{T_1 T_2}\right) + \dot{m}\left(\frac{g_2}{T_2} - \frac{g_1}{T_1}\right). \tag{53}$$

Since the temperatures are in equilibrium by the temperature relaxation the first term in the right hand side of (53) vanishes and the mass transfer is modeled as $\dot{m} = \nu(g_2 - g_1)$, where $\nu > 0$ is the relaxation parameter of the Gibbs free energy. Thus the mixture entropy satisfies the second law of thermodynamics, i.e.

$$\frac{\partial \rho s}{\partial t} + \frac{\partial \rho s u}{\partial x} = \nu \frac{(g_2 - g_1)^2}{T_{eq}} \geqslant 0, \tag{54}$$

where T_{eq} is the equilibrium temperature, $T_1 = T_2 = T_{eq}$.

In this work we assume that the parameter v tends to infinity. This means that the Gibbs free energy relaxes instantaneously to equilibrium. This is considered at the interface only.

4.2.3. Free Gibbs energy relaxation, procedure I

Now, we will solve the system (37) when $v \to \infty$, this means that the mass transfer occurs until the Gibbs free energies reach equilibrium. Thus we have to find the value of $\dot{m}$ that makes the difference of the Gibbs free energies at the end of the time step is zero. To do that we use the equations for the rate of change of Gibbs free energies in terms of $\dot{m}$. Assume that

$$\frac{\partial g_1}{\partial t} = A\dot{m}, \quad \text{and} \quad \frac{\partial g_2}{\partial t} = B\dot{m}. \tag{55}$$

Using the SG-EOS, A and B can be given as

$$\begin{aligned} A &= \frac{\gamma_1 C_{v1} - C_{v1} - s_1}{\alpha_1 \rho_1 \varrho C_{v1}}[(e_1 - q_1)(\varrho - \rho_1) + \varrho(e_i - e_1)] \\ &\quad + \left[T_1(s_1 + \gamma_1 C_{v1}) - \frac{p_1}{\rho_1} - (e_1 - q_1)\right]\frac{(\varrho - \rho_1)}{\alpha_1 \rho_1 \varrho}, \\ B &= -\frac{\gamma_2 C_{v2} - C_{v2} - s_2}{\alpha_2 \rho_2 \varrho C_{v2}}[(e_2 - q_2)(\varrho - \rho_2) + \varrho(e_i - e_2)] - \left[T_2(s_2 + \gamma_2 C_{v2}) - \frac{p_2}{\rho_2} - (e_2 - q_2)\right]\frac{(\varrho - \rho_2)}{\alpha_2 \rho_2 \varrho}. \end{aligned}$$

From (55) we get

$$\frac{\partial \Delta g}{\partial t} = \frac{\partial (g_1 - g_2)}{\partial t} = (A - B)\dot{m}.$$

The simplest numerical approximation of this equation is

$$\frac{(\Delta g)^{n+1} - (\Delta g)^n}{\Delta t} = (A - B)^n (\dot{m})^n.$$

To satisfy the equilibrium condition for the Gibbs free energies we require $(\Delta g)^{n+1} = 0$. Thus the mass transfer can be approximated as

$$(\dot{m})^n = \frac{-(\Delta g)^n}{\Delta t (A - B)^n}.$$

Using this approximation for $(\dot{m})^n$ we can integrate the system (37). But we may face the problem of loosing the positivity of the volume fraction. Therefore a limitation on the value $\dot{m}/\varrho$ must be used. We take the following procedure from [33] which we cite for the sake of completeness. Assume that $S_{\alpha_1} = \dot{m}/\varrho$. Then the maximum admissible source term for the volume fraction evolution in order to preserve the positivity is given as

$$S_{max,\alpha_1} = \begin{cases} \frac{1-\alpha_1}{\Delta t}, & S_{\alpha_1} > 0, \\ -\frac{\alpha_1}{\Delta t}, & \text{otherwise}. \end{cases} \tag{56}$$

Then, if $|S_{\max,\alpha_1}| > |S_{\alpha_1}|$, the numerical integration for the system (37) can be done with the hydrodynamics time step which is restricted by the CFL number. Otherwise, the integration time step has to be reduced. The ratio $R_{\alpha_1} = S_{\max,\alpha_1}/S_{\alpha_1}$ is computed and the system (37) is integrated over a fraction of the time step, typically $\Delta t_m = R_{\alpha_1}\Delta t/2$. Successive point integrations are done to cover the complete hydrodynamic step.

The above procedure is cheap, fast and easy to implement. But this procedure is not an instantaneous one. This means that the equilibrium of the Gibbs free energy is reached very fast after a very short time but not instantaneously. Hereafter we propose another method for the Gibbs free energy relaxation which is an instantaneous relaxation procedure.

4.2.4. Free Gibbs energy relaxation, procedure II

By considering (37b) and (37c) with the fact that the velocities are in equilibrium we get $\frac{\partial u_1}{\partial t} = 0$. Using this with (37c) and (37d) we get

$$\frac{\partial \alpha_1 \rho_1 e_1}{\partial t} = e_i \dot{m}. \tag{57}$$

From (57) with (37a) we have

$$\frac{\partial \alpha_1 \rho_1 e_1}{\partial t} = \varrho e_i \frac{\partial \alpha_1}{\partial t}. \tag{58}$$

Integrating (58) we get the following approximation

$$(\alpha_1 \rho_1 e_1)^* = (\alpha_1 \rho_1 e_1)^0 + \overline{\varrho e}_i(\alpha_1^* - \alpha_1^0), \tag{59}$$

where $\overline{\varrho e}_i$ is the mean interfacial value between the states $(\alpha_1^0, \rho_1^0, e_1^0)$ and $(\alpha_1^*, \rho_1^*, e_1^*)$.

From (37a) and (37b) we have

$$\frac{\partial \alpha_1\rho_1}{\partial t} = \varrho \frac{\partial \alpha_1}{\partial t}.$$

Integrating this equation we get

$$(\alpha_1\rho_1)^* = (\alpha_1\rho_1)^0 + \bar{\varrho}(\alpha_1^* - \alpha_1^0), \tag{60}$$

where $\bar{\varrho}$ is the mean interfacial value between the states $(\alpha_1^0, \rho_1^0, e_1^0)$ and $(\alpha_1^*, \rho_1^*, e_1^*)$.

In the same way we have the following equations for phase '2'

$$(\alpha_2\rho_2 e_2)^* = (\alpha_2\rho_2 e_2)^0 - \overline{\varrho e}_i(\alpha_1^* - \alpha_1^0), \tag{61}$$

$$(\alpha_2\rho_2)^* = (\alpha_2\rho_2)^0 - \bar{\varrho}(\alpha_1^* - \alpha_1^0). \tag{62}$$

Eq. (60) shows that the density ρ_1 is a function of α_1. Using this fact with (59) we conclude that e_1 is also a function of α_1. Analogously ρ_2 and e_2 are functions of α_1. We aim now to find the α_1 which satisfies the equilibrium condition

$$f_g(\alpha_1) = g_2(e_2, \rho_2) - g_1(e_1, \rho_1) = 0. \tag{63}$$

The Eq. (63) can be solved by any iterative procedure. In this way the Gibbs free energy equilibrium is reached instantaneously.

This procedure for the Gibbs free energy relaxation is more expensive since an iterative method is used, but this method has a better resolution than the previous procedure.

4.3. The final model

In result of this section, the full model with heat and mass transfer is given as

$$\frac{\partial \alpha_1}{\partial t} + u_I \frac{\partial \alpha_1}{\partial x} = \mu(p_1 - p_2) + \frac{Q}{\kappa} + \frac{\dot{m}}{\varrho}, \tag{64a}$$

$$\frac{\partial \alpha_1\rho_1}{\partial t} + \frac{\partial(\alpha_1\rho_1 u_1)}{\partial x} = \dot{m}, \tag{64b}$$

$$\frac{\partial \alpha_1\rho_1 u_1}{\partial t} + \frac{\partial(\alpha_1\rho_1 u_1^2 + \alpha_1 p_1)}{\partial x} = p_I \frac{\partial \alpha_1}{\partial x} + \lambda(u_2 - u_1) + u_I\dot{m}, \tag{64c}$$

$$\frac{\partial \alpha_1\rho_1 E_1}{\partial t} + \frac{\partial(\alpha_1(\rho_1 E_1 + p_1)u_1)}{\partial x} = p_I u_I \frac{\partial \alpha_1}{\partial x} + \mu p_I(p_2 - p_1) + \lambda u_I(u_2 - u_1) + Q + \left(e_i + \frac{u_I^2}{2}\right)\dot{m}, \tag{64d}$$

$$\frac{\partial \alpha_2\rho_2}{\partial t} + \frac{\partial(\alpha_2\rho_2 u_2)}{\partial x} = -\dot{m}, \tag{64e}$$

$$\frac{\partial \alpha_2\rho_2 u_2}{\partial t} + \frac{\partial(\alpha_2\rho_2 u_2^2 + \alpha_2 p_2)}{\partial x} = -p_I \frac{\partial \alpha_1}{\partial x} - \lambda(u_2 - u_1) - u_I\dot{m}, \tag{64f}$$

$$\frac{\partial \alpha_2\rho_2 E_2}{\partial t} + \frac{\partial(\alpha_2(\rho_2 E_2 + p_2)u_2)}{\partial x} = -p_I u_I \frac{\partial \alpha_1}{\partial x} - \mu p_I(p_2 - p_1) - \lambda u_I(u_2 - u_1) - Q - \left(e_i + \frac{u_I^2}{2}\right)\dot{m}, \tag{64g}$$

where

$$Q = \theta(T_2 - T_1),$$
$$\dot{m} = \nu(g_2 - g_1).$$

The variables κ, ϱ and e_i are given in (30), (49a) and (49b) respectively. All relaxation parameters λ, μ, θ and ν are assumed to be infinite. The model (64) is solved by the Strang splitting (9). The operator L_s approximates the solution of the ordinary differential system (20). This system is solved by successive integrations considering separately each one of the source vectors that are related to the relaxation of the velocity, pressure, temperature and Gibbs free energy. The order of the successive integrations are essential for our model. They are done firstly for the velocity relaxation, then for the pressure relaxation, after for the temperature relaxation and finally for the Gibbs free energy relaxation. The velocity and the pressure relaxation are performed for the entire flow field while the temperature and the Gibbs free energy relaxation are used at the interface only. For the hyperbolic operator L_h a Godunov-type scheme is used.

5. Modeling phase transition for the six-equation model

The six-equation model with a single velocity is obtained from the seven-equation model in the asymptotic limit of zero velocity relaxation time, see Kapila et al. [15]. This model, as the seven-equation model, has more attractive advantages over the five-equation model for the numerical computations. Also this model is less expensive than the seven-equation model.

In this section we will insert the heat and mass transfer in the six-equation model by the relaxation effects. The above assumptions and ideas for the seven-equation model will be used, i.e. we will assume that the pressure relaxes much faster than the thermal properties and the temperature relaxation time is much smaller than that of the Gibbs free energy.

The six-equation model without heat and mass transfer can be written as

$$\frac{\partial \alpha_1}{\partial t} + u\frac{\partial \alpha_1}{\partial x} = \mu(p_1 - p_2), \tag{65a}$$

$$\frac{\partial \alpha_1\rho_1}{\partial t} + \frac{\partial(\alpha_1\rho_1 u)}{\partial x} = 0, \tag{65b}$$

$$\frac{\partial \alpha_2\rho_2}{\partial t} + \frac{\partial(\alpha_2\rho_2 u)}{\partial x} = 0, \tag{65c}$$

$$\frac{\partial \rho u}{\partial t} + \frac{\partial(\rho u^2 + \alpha_1 p_1 + \alpha_2 p_2)}{\partial x} = 0, \tag{65d}$$

$$\frac{\partial \alpha_1\rho_1 e_1}{\partial t} + \frac{\partial \alpha_1\rho_1 e_1 u}{\partial x} + \alpha_1 p_1 \frac{\partial u}{\partial x} = \mu p_I(p_2 - p_1), \tag{65e}$$

$$\frac{\partial \alpha_2\rho_2 e_2}{\partial t} + \frac{\partial \alpha_2\rho_2 e_2 u}{\partial x} + \alpha_2 p_2 \frac{\partial u}{\partial x} = -\mu p_I(p_2 - p_1). \tag{65f}$$

In this section we use the relation (3) for the interfacial pressure p_I.

We apply the idea of Saurel et al. [34] that during the numerical computations we use the mixture energy equation to correct the thermodynamic state predicted by the two non-conservative internal energy equations. By summing the two internal energy equations and using the mass and momentum equations we obtain the mixture energy equation

$$\frac{\partial\left(\rho e + \frac{1}{2}\rho u^2\right)}{\partial t} + \frac{\partial u\left(\rho e + \frac{1}{2}\rho u^2 + \alpha_1 p_1 + \alpha_2 p_2\right)}{\partial x} = 0. \tag{66}$$

where $\rho = \alpha_1\rho_1 + \alpha_2\rho_2$ and $\rho e = \alpha_1\rho_1 e_1 + \alpha_2\rho_2 e_2$.

5.1. Mathematical properties of the six-equation model

In terms of the primitive variables $\mathbf{W} = (\alpha_1, \rho_1, \rho_2, u, p_1, p_2)$, the model (65) can be expressed as

$$\frac{\partial \mathbf{W}}{\partial t} + \mathbf{A}\frac{\partial \mathbf{W}}{\partial x} = \mathbf{S} \tag{67}$$

where the matrix $\mathbf{A}$ is given as

$$\mathbf{A} = \begin{bmatrix} u & 0 & 0 & 0 & 0 & 0 \\ 0 & u & 0 & \rho_1 & 0 & 0 \\ 0 & 0 & u & \rho_2 & 0 & 0 \\ \frac{p_1-p_2}{\rho} & 0 & 0 & u & \frac{\alpha_1}{\rho} & \frac{1-\alpha_1}{\rho} \\ 0 & 0 & 0 & \rho_1 c_1^2 & u & 0 \\ 0 & 0 & 0 & \rho_2 c_2^2 & 0 & u \end{bmatrix}.$$

The matrix $\mathbf{A}$ has six eigenvalues, only three of them are distinct

$$\begin{aligned} &\lambda_1 = \lambda_2 = \lambda_3 = \lambda_4 = u, \\ &\lambda_5 = u + c, \\ &\lambda_6 = u - c. \end{aligned} \tag{68}$$

Here c is the *mixture sound speed* and is expressed as

$$c^2 = \frac{\alpha_1\rho_1}{\rho}c_1^2 + \frac{\alpha_2\rho_2}{\rho}c_2^2.$$

The sound speeds $c_k, k = 1, 2$, are defined by (4).

The corresponding right eigenvectors are

$$\mathbf{r}_1 = \begin{bmatrix} 0 \\ 0 \\ 0 \\ 0 \\ -\frac{\alpha_2}{\alpha_1} \\ 1 \end{bmatrix}, \quad \mathbf{r}_2 = \begin{bmatrix} 0 \\ 0 \\ 1 \\ 0 \\ 0 \\ 0 \end{bmatrix}, \quad \mathbf{r}_3 = \begin{bmatrix} 0 \\ 1 \\ 0 \\ 0 \\ 0 \\ 0 \end{bmatrix}, \quad \mathbf{r}_4 = \begin{bmatrix} 1 \\ 0 \\ 0 \\ 0 \\ \frac{p_2-p_1}{\alpha_1} \\ 0 \end{bmatrix}, \quad \mathbf{r}_5 = \begin{bmatrix} 0 \\ 1 \\ \frac{\rho_2}{\rho_1} \\ \frac{c}{\rho_1} \\ c_1^2 \\ \frac{\rho_2}{\rho_1}c_2^2 \end{bmatrix}, \quad \mathbf{r}_6 = \begin{bmatrix} 0 \\ 1 \\ \frac{\rho_2}{\rho_1} \\ -\frac{c}{\rho_1} \\ c_1^2 \\ \frac{\rho_2}{\rho_1}c_2^2 \end{bmatrix}. \tag{69}$$

Therefore, the system (65) is hyperbolic, but not strictly hyperbolic.

5.2. Numerical method

To take into account the non-differential source terms the Strang splitting (9) is used. In this case the vector of conservative variables **U** is given as

$$\mathbf{U} = \left(\alpha_1, \alpha_1\rho_1, \alpha_2\rho_2, \rho u, \alpha_1\rho_1 e_1, \alpha_2\rho_2 e_2, \rho e + \frac{1}{2}\rho u^2\right)^T.$$

The last element in **U** corresponds to the redundant Eq. (66).

For the hyperbolic part of the system a Godunov-type scheme is used that takes into account the discretization of the non-conservative terms.

The source vector **S** is associated with the relaxation terms and is decomposed as

$$\mathbf{S} = \mathbf{S}_P + \mathbf{S}_Q + \mathbf{S}_m,$$

where $\mathbf{S}_P = (\mu(p_1 - p_2), 0, 0, 0, \mu p_I(p_2 - p_1), -\mu p_I(p_2 - p_1), 0)^T$ represents the pressure relaxation terms. The vectors $\mathbf{S}_Q$ and $\mathbf{S}_m$ are associated with the heat and mass transfer relaxation terms respectively, they will be considered in the next section.

The HLL, HLLC and VFRoe Riemann solvers can be used. For the HLL solver we refer to the book of Toro [38], it is detailed in the context of Euler equations there but it is easily modified to the six-equation model. The HLLC solver was introduced above in Section 3.1.1 for the seven-equation model and is detailed in Ref. [34] for the six-equation model. The VFRoe solver [12] is explained in the following section in the context of the six-equation model.

5.2.1. VFRoe-type solver

Consider the Riemann problem consists of the homogenous part of the system (67)

$$\frac{\partial \mathbf{W}}{\partial t} + \mathbf{A}\frac{\partial \mathbf{W}}{\partial x} = 0,$$

with the initial conditions

$$\mathbf{W}(x,0) = \begin{cases} \mathbf{W}_L, & x < 0, \\ \mathbf{W}_R, & x > 0. \end{cases}$$

The Jacobian matrix $A(\overline{\mathbf{W}})$ is calculated in the average state

$$\overline{\mathbf{W}} = \frac{\mathbf{W}_L + \mathbf{W}_R}{2}.$$

The intermediate state in the solution of the Riemann problem is

$$\mathbf{W}^* = \mathbf{W}_L + \sum_{\lambda_i < 0} a_i \mathbf{r}_i,$$

where the eigenvalues λ_i and the corresponding eigenvectors $\mathbf{r}_i$ are given by (68) and (69).

The coefficients a_i are determined by

$$\mathbf{W}_R - \mathbf{W}_L = \sum_{i=1}^{6} a_i \mathbf{r}_i,$$

Indeed, they are given by the following expressions

$$a_4 = \Delta_1,$$

$$a_1 = -\frac{\frac{\rho_2}{\rho_1}c_2^2\Delta_5 - c_1^2\Delta_6 - \frac{\rho_2 c_2^2 a_4(p_2 - p_1)}{\alpha_1\rho_1}}{\frac{\alpha_2\rho_2}{\alpha_1\rho_1}c_2^2 + c_1^2},$$

$$a_5 = \frac{\rho_1\rho_2 c_2^2\Delta_4 + \rho_1 c\Delta_6 - \rho_1 c a_1}{2\rho_2 c c_2^2},$$

$$a_6 = a_5 - \frac{\rho_1}{c}\Delta_4,$$

$$a_2 = \Delta_3 - \frac{\rho_2}{\rho_1}(a_5 + a_6),$$

$$a_3 = \Delta_2 - a_5 - a_6,$$

where Δ_k is the kth component of $\mathbf{W}_R - \mathbf{W}_L = (\Delta_1, \ldots, \Delta_6)^T$.

5.2.2. Godunov-type method

The equations that are written in a conservative form are discretized by the conventional Godunov scheme

$$\mathbf{u}_j^{n+1} = \mathbf{u}_j^n - \frac{\Delta t}{\Delta x}[\mathbf{f}(\mathbf{u}^*(\mathbf{u}_j^n, \mathbf{u}_{j+1}^n)) - \mathbf{f}(\mathbf{u}^*(\mathbf{u}_{j-1}^n, \mathbf{u}_j^n))],$$

where

$$\mathbf{u} = (\alpha_1\rho_1, \alpha_2\rho_2, \rho u, \rho e + \frac{1}{2}\rho u^2)^T$$

and

$$\mathbf{f}(\mathbf{u}) = (\alpha_1\rho_1 u, \alpha_2\rho_2 u, \rho u^2 + \alpha_1 p_1 + \alpha_2 p_2, u(\rho e + \frac{1}{2}\rho u^2 + \alpha_1 p_1 + \alpha_2 p_2))^T.$$

The volume fraction equation and the internal energy equations are discretized as, see [34],

$$\alpha_{1j}^{n+1} = \alpha_{1j}^n - \frac{\Delta t}{\Delta x}\left((u\alpha_1)_{j+\frac{1}{2}}^* - (u\alpha_1)_{j-\frac{1}{2}}^* - \alpha_{1j}^n\left(u_{j+\frac{1}{2}}^* - u_{j-\frac{1}{2}}^*\right)\right),$$
$$(\alpha\rho e)_{kj}^{n+1} = (\alpha\rho e)_{kj}^n - \frac{\Delta t}{\Delta x}\left((\alpha\rho e u)_{kj+\frac{1}{2}}^* - (\alpha\rho e u)_{kj-\frac{1}{2}}^* + (\alpha p)_{kj}^n\left(u_{j+\frac{1}{2}}^* - u_{j-\frac{1}{2}}^*\right)\right).$$

To achieve a second-order accuracy we use the MUSCL method detailed in Section 3.1.2.

5.2.3. Pressure relaxation and the correction criterion

It is clear that the pressure relaxation procedure for the seven-equation model that is introduced in [27] can be easily used for the six-equation model. Also we refer to the relaxation procedure that is used in Ref. [34]. We see that there is no significant difference between the results of the two procedures in our numerical results.

To make the relaxed pressure in agreement with the mixture EOS a correction criterion of [34] is used. From the SG-EOS (5a) for each phase with the pressure equilibrium we obtain the following expression for the mixture EOS, see [33,34]

$$p(\rho_1, \rho_2, e, \alpha_1) = \frac{\rho e - \alpha_1\rho_1 q_1 - \alpha_2\rho_2 q_2 - \left(\frac{\alpha_1\gamma_1\pi_1}{\gamma_1 - 1} + \frac{\alpha_2\gamma_2\pi_2}{\gamma_2 - 1}\right)}{\frac{\alpha_1}{\gamma_1 - 1} + \frac{\alpha_2}{\gamma_2 - 1}}. \tag{70}$$

The mixture pressure (70) is obtained from the evolution of the mixture total energy (66). This is expected to be accurate in the entire field flow since the Eq. (66) is written in the conservative formulation.

By using evolution of the mixture total energy (66) we can find the value of ρe. Using this value in (70) we can find the value of the mixture pressure. Other variables in the relation (70) are estimated by the relaxation step. In this way we determine the value of the mixture pressure that agrees with the mixture EOS, then we use this value with the SG-EOS for each phase to reset the values of the internal energies.

5.3. Modeling of the heat and mass transfer for the six-equation model

To take into account the heat and mass transfer we have to solve the following system of ODE at each time step after the pressure relaxation step

$$\frac{d\mathbf{U}}{dt} = \mathbf{S}_Q + \mathbf{S}_m. \tag{71}$$

The system (71) is solved by considering each one of the source vectors alone. According to our assumptions during the temperature relaxation the pressures will stay in equilibrium, i.e. the condition (23) holds. And during the Gibbs free energy relaxation the pressures and the temperatures will stay in equilibrium, i.e. the conditions (38) hold.

The heat source vector is modeled as

$$\mathbf{S}_Q = \left(\frac{Q}{\kappa}, 0, 0, 0, Q, -Q, 0\right)^T, \tag{72}$$

where $Q = \theta(T_2 - T_1)$. Note that the last element of $\mathbf{S}_Q$ corresponds to the redundant Eq. (66). It is clear that the value of κ (30) for the seven-equation model works also for the six-equation model and satisfies the condition (23). Also it is easy to see that the same method of temperature relaxation for the seven-equation model can be used for the six-equation model.

The vector $\mathbf{S}_m$ is modeled as

$$\mathbf{S}_m = \left(\frac{\dot{m}}{\varrho}, \dot{m}, -\dot{m}, 0, e_i\dot{m}, -e_i\dot{m}, 0\right), \tag{73}$$

where $\dot{m} = \nu(g_2 - g_1)$. The values of ϱ and e_i that satisfy the conditions (38) are given in (49). Also the Gibbs free energy relaxation procedures for the seven-equation model can be used directly here.

Thus the final six-equation model with heat and mass transfer is given as

$$\frac{\partial \alpha_1}{\partial t} + u\frac{\partial \alpha_1}{\partial x} = \mu(p_1 - p_2) + \frac{1}{\kappa}Q + \frac{1}{\varrho}\dot{m}, \tag{74a}$$

$$\frac{\partial \alpha_1\rho_1}{\partial t} + \frac{\partial(\alpha_1\rho_1 u)}{\partial x} = \dot{m}, \tag{74b}$$

$$\frac{\partial \alpha_2\rho_2}{\partial t} + \frac{\partial(\alpha_2\rho_2 u)}{\partial x} = -\dot{m}, \tag{74c}$$

$$\frac{\partial \rho u}{\partial t} + \frac{\partial(\rho u^2 + \alpha_1 p_1 + \alpha_2 p_2)}{\partial x} = 0, \tag{74d}$$

$$\frac{\partial \alpha_1\rho_1 e_1}{\partial t} + \frac{\partial \alpha_1\rho_1 e_1 u}{\partial x} + \alpha_1 p_1 \frac{\partial u}{\partial x} = \mu p_I(p_2 - p_1) + Q + e_i\dot{m}, \tag{74e}$$

$$\frac{\partial \alpha_2\rho_2 e_2}{\partial t} + \frac{\partial \alpha_2\rho_2 e_2 u}{\partial x} + \alpha_2 p_2 \frac{\partial u}{\partial x} = -\mu p_I(p_2 - p_1) - Q - e_i\dot{m}. \tag{74f}$$

On the other hand, the six-equation model with heat and mass transfer is obtained directly from the seven-equation model involving the heat and mass transfer by the limit of infinitely fast velocity relaxation. This is shown in the Appendix B. We apply the reduction method of Chen et al. [6] on the seven-equation model including the heat and mass transfer (64) assuming stiff velocity relaxation. The resulting model is the six-equation model (74).

6. Numerical results

The tests for metastable liquids in Ref. [33] are used.

6.1. Two-phase shock tube

Consider a 1 m shock tube filled with liquid dodecane under high pressure at the left, and with the vapor dodecane at atmospheric pressure at the right. The initial discontinuity is set at 0.75 m, and the initial data are

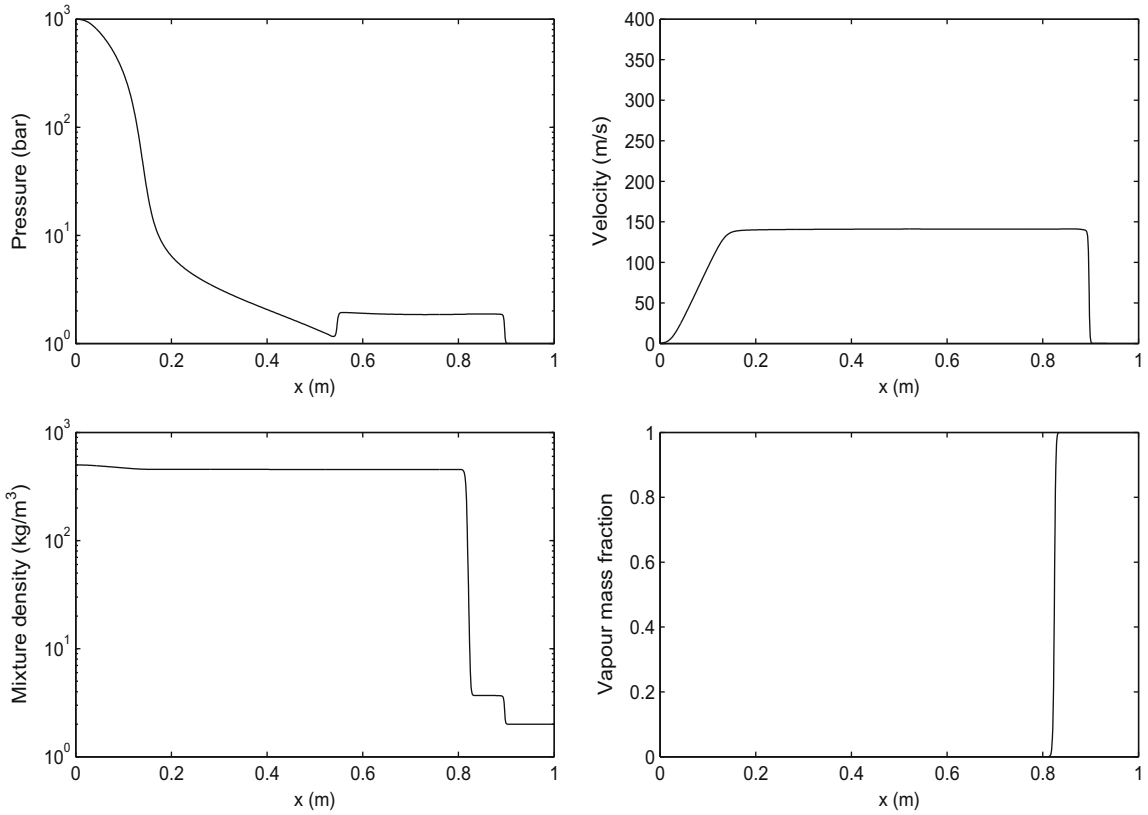

Fig. 1. Dodecane liquid–vapor shock tube without phase transition, by using the seven-equation model. The mesh involves 1250 cells, the CPU time is 100.65 s and the number of time steps is 7197. The scale for the velocity graph is chosen in this way for a direct comparison with the velocity graph in Fig. 2.

$$\text{Left}: \quad p_l = 10^8 \text{ Pa}, \quad \rho_l = 500 \text{ kg/m}^3, \quad u_l = 0 \text{ m/s}$$
$$\text{Right}: \quad p_v = 10^5 \text{ Pa}, \quad \rho_v = 2 \text{ kg/m}^3, \quad u_v = 0 \text{ m/s}.$$

For numerical reasons, in each side of the shock tube we allow the presence of a small volume fraction of the other fluid, typically 10^{-6}.

All computations for this example were done with a CFL number of 0.6. They used the first Gibbs free energy relaxation procedure with a limitation on the source terms given by (56). The time step for the fluid motion is restricted by the CFL number, but we observed that the Gibbs free energy relaxation procedure may require smaller time to ensure the positivity of the volume fraction. This means that sometimes the Eqs. (37) are stiff. Thus by using the limitation (56) a smaller time step is used for the Gibbs free energy relaxation procedure and successive point integrations are done to cover the complete hydrodynamic step that is restricted by the CFL number. In the presence of stiffness from the Gibbs free energy relaxation, the first Gibbs free energy relaxation procedure is more appropriate than the second relaxation procedure, this is due to the easy of impostion the limitation (56) on the source terms.

By using the seven-equation model the results are shown at time $t = 473$ μs. Fig. 1 gives the results without phase transition, while in Fig. 2 we see the case when the phase transition is included.

In comparison between the two figures, an extra wave appears between the rarefaction wave and the contact discontinuity which corresponds the evaporation front. Indeed, rarefaction waves propagate through the liquid producing a superheated liquid and evaporation has occurred. An extra wave representing the evaporation front propagates through the superheated liquid and produces a liquid vapor mixture at thermodynamic equilibrium with a high velocity, for more details see [33].

A comparison between the results of the six-equation model and the seven-equation model is shown in Figs. 3–6 by using the same number of cells and the same type of the Riemann solver. It is clear that for both cases, with or without the phase transition, the results almost coincide. Just a very small difference appears at the left rarefaction in the curves of the pressure. Such a small difference has no significant numerical meaning. This small difference appears in both cases i.e. with or without the phase transition in the same manner, see the pressure profiles on logarithmic scales, Figs. 4 and 5, the pressure profiles are drawn separately to be able to see the differences. Thus this small difference is not related to the treatment of the phase transition.

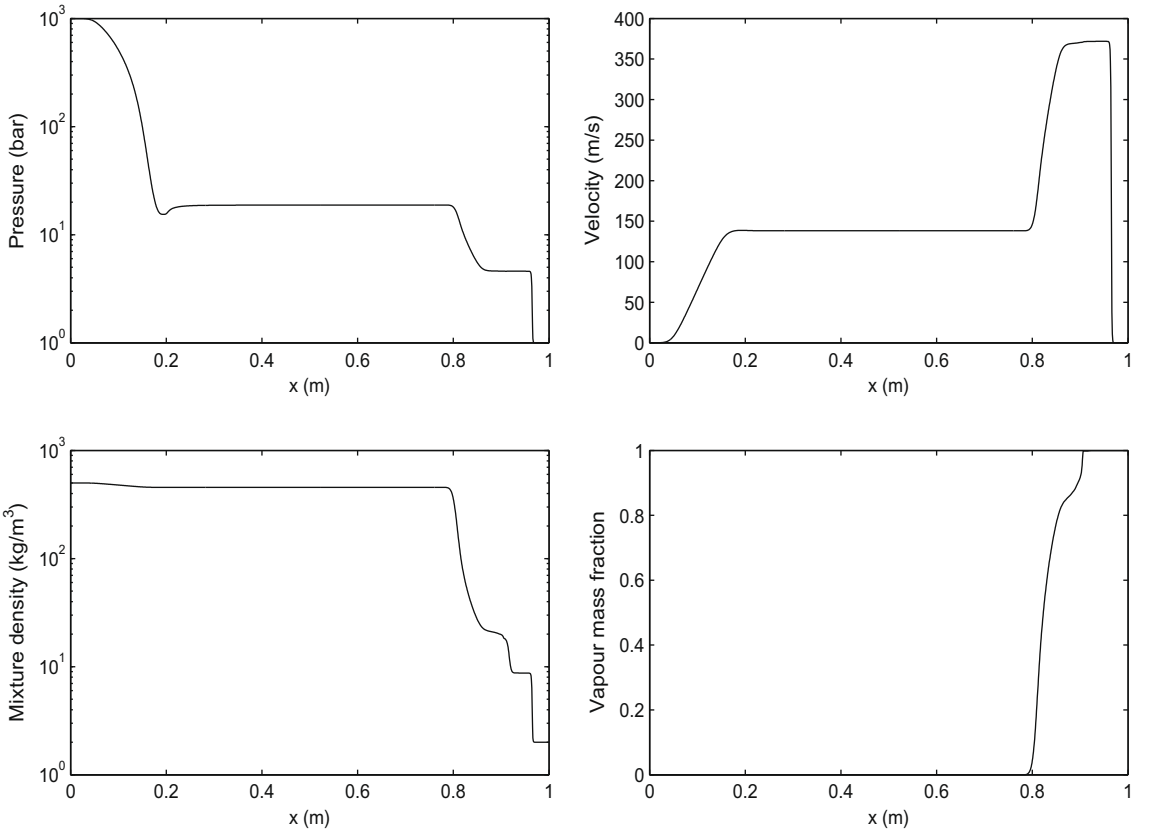

Fig. 2. Dodecane liquid–vapor shock tube with phase transition, by using the seven-equation model. The mesh involves 1250 cells, the CPU time is 151.98 s and the number of time steps is 8828.

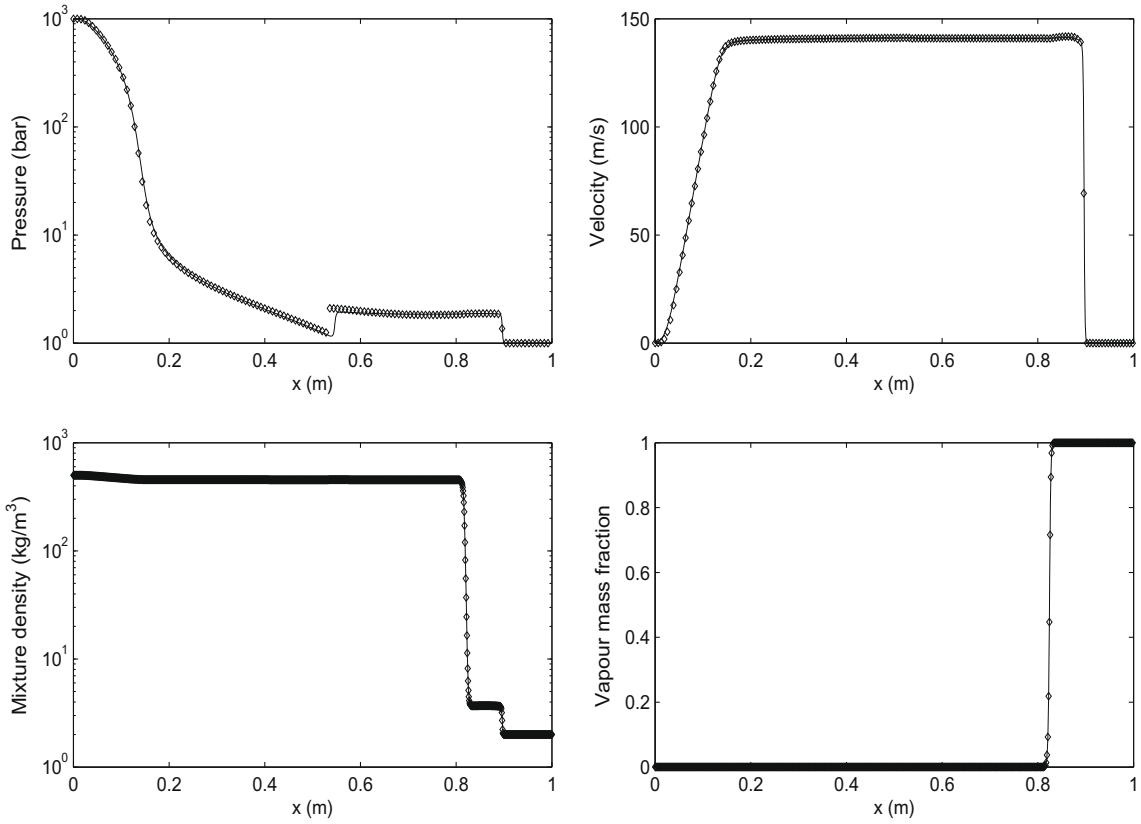

Fig. 3. Dodecane liquid–vapor shock tube without phase transition, a comparison between the results of the seven-equation model (lines) and the six-equation model results (symbols). The computations used 1250 cells. For the seven-equation model results: The CPU time is 100.65 s with 7197 time steps. For the six-equation model results: The CPU time is 14.46 s with 1557 time steps.

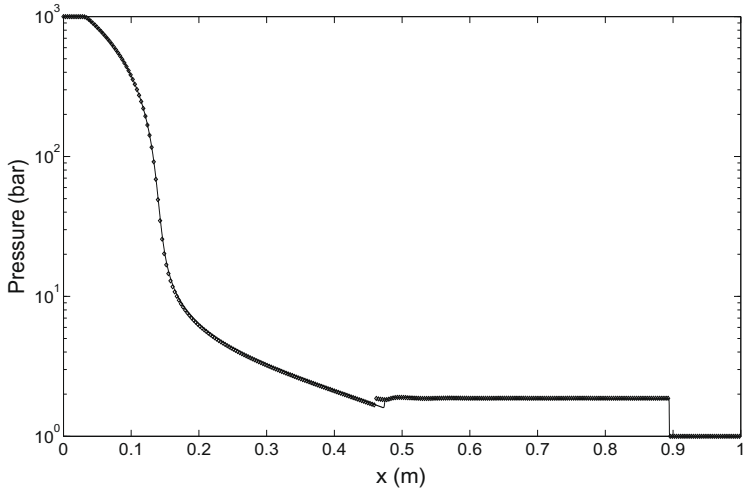

Fig. 4. Dodecane liquid–vapor shock tube without phase transition. The pressure profile over (10,000) cells, by the seven-equation model (lines) and the six-equation model (symbols). For the seven-equation model: The CPU time is 8145.17 s taking 56,749 time steps. For the six-equation model: The CPU time is 1035.01 s with 12,452 time steps.

At the right face of the left rarefaction wave in the pressure profile in Figs. 2 and 5 we can see a small distortion which does not appear in the results of Saurel et al. [33] by using the five-equation model. We reran this test for higher number of cells for both models, seven-equation and six-equation, but observed no change. In fact we see the same feature on the curve

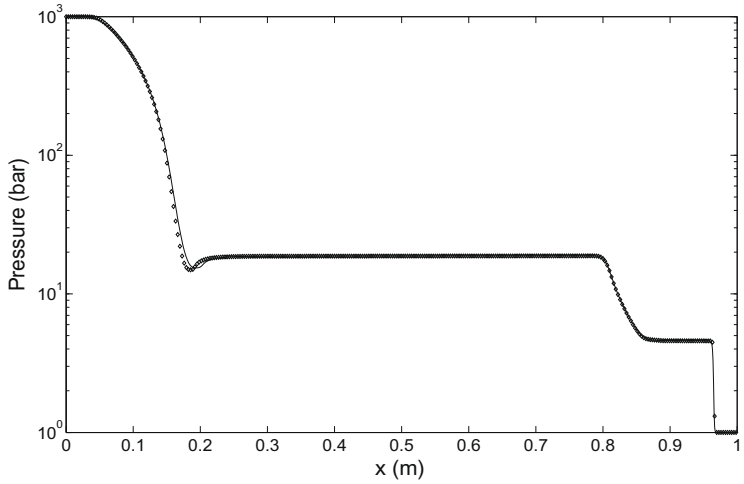

Fig. 5. Dodecane liquid–vapor shock tube with phase transition. The pressure profile, a comparison between the results of the seven-equation model (lines) and the six-equation model results (symbols). The computations were done with 1250 cells. For the seven-equation model: The CPU time is 151.98 s with 8828 time steps. For the six-equation model: The CPU time is 19.87 s with 1556 time steps.

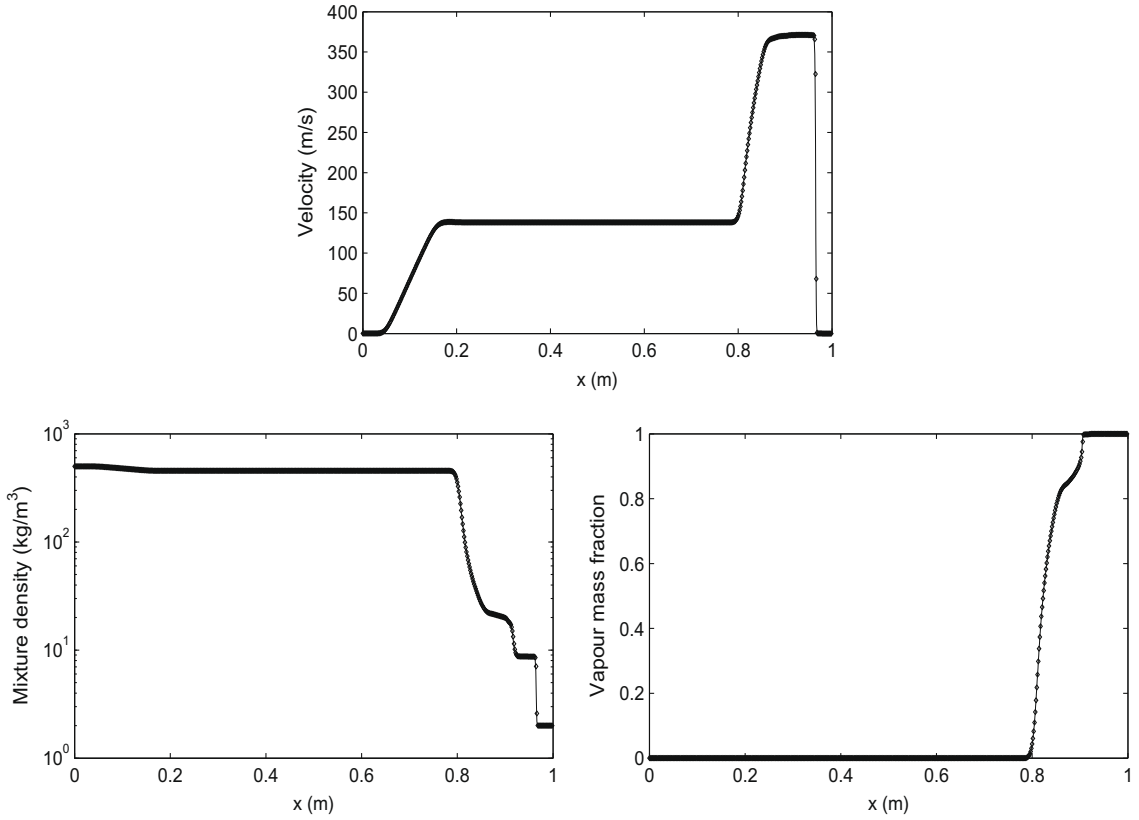

Fig. 6. Dodecane liquid–vapor shock tube with phase transition, a comparison between the results of the seven-equation model (lines) and the six-equation model results (symbols). The computations used 1250 cells. For the seven-equation model: The CPU time is 151.98 s with 8828 time steps. For the six-equation model: The CPU time is 19.87 s with 1556 time steps.

of the pressure without phase transition, see Fig. 4. The pressure curve is shown on logarithmic scale, 10,000 cells were used in the computations but this distortion still appears. Thus we conclude that this is not related to our new modifications for

heat and mass transfer. This may come from the nature of the initial seven-equation or six-equation model or from the numerical method without phase transition. Moreover, such differences between the results of the seven-equation model and the five-equation model without phase transition appear also in the results of [23]. This requires further investigation.

In result, for this example, we see that there is no significant difference between the results of the seven-equation model and the six-equation model and both models give similar results. But there is a significant difference in the required CPU time. The required time for the six-equation model is much smaller ($\approx 13\%$) than that required for the seven-equation model.

6.2. Validation against shock tube experiments

Experimental results were obtained by Simões-Moreira and Shepherd [36]. Liquid dodecane in a tube was suddenly expanded into a low pressure chamber (1 mbar). An evaporation front or wave propagated into metastable liquid with a steady mean velocity. This velocity was measured for different initial temperatures of liquid dodecane. Also pressure data were obtained during the evaporation event before and after the evaporation wave, see [36] and for full details see the Ph.D. Thesis of Simões-Moreira [35].

At each temperature we compute the front velocity under conditions which are close to the experimental conditions with help of Le Metayer et al. [21]. We consider a low pressure chamber (1 mbar) filled with gaseous dodecane at right side of the shock tube with density 10^{-4} kg/m^3. While a liquid dodecane is considered initially at the left side of the shock tube with a higher pressure. We adjust the initial pressure of the left hand side, so that the pressure in the state before the evaporation front is equal to the measured value. The density of the liquid is calculated from the equation of state (5b), as the initial temperature is known.

Table 3 shows the estimated initial pressure that we use for each temperature, column two. The columns three and four represent the experimental data for the pressure before the evaporation wave and the front velocity respectively [36]. The fifth column shows the computed values for the front velocity by present model.

Table 3
Estimated initial pressure, experimental results and the computed front velocity at several initial temperatures.

T_l (K)	p_l (bar)	p_B (bar)	U_F (m/s) (measured)	U_F (m/s) (computed)
453	1.5	0.24	0.253	0.147
473	2.2	0.33	0.309	0.240
489	3.0	0.44	0.390	0.328
503	3.9	0.59	0.472	0.441
523	5.0	0.83	0.648	0.576
543	7.5	1.19	0.837	0.888
563	11.0	1.91	1.381	1.337
573	13.0	2.12	1.578	1.620

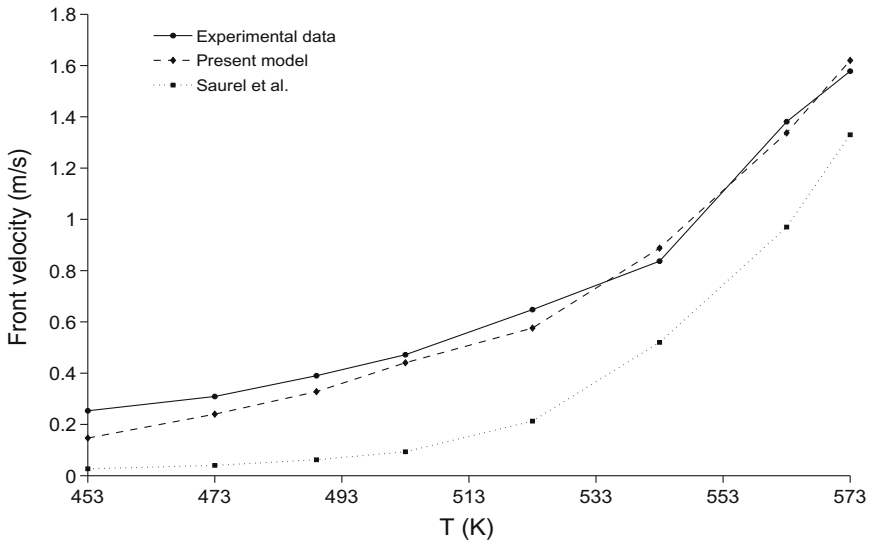

Fig. 7. Evaporation front velocity versus initial temperature of liquid dodecane. Comparison between our results with the experimental results of Simões-Moreira and Shepherd [36] and the computed results of Saurel et al. [33].

As in [33] the front velocity is computed as a local wave speed, i.e. $U_F = ((\rho u)_i - (\rho u)_{i-1})/(\rho_i - \rho_{i-1})$, where i refers to the state after the evaporation wave. The computed values for the front velocity are calculated at several time ponits in the range between 200 μs and 500 μs. Then an averaged value is taken. We see that for each case the computed values at different times are very close.

A comparison between our results with the experimental results and the results of Saurel et al. [33] is shown in Fig. 7. It is clear that our results are more close to the experimental results. There is still not perfect agreement with the experimental data. This is related to several sources, like how realistic the equations of state we used are and how close we are to the real initial conditions of the experiments. However we have a reasonable agreement with the experimental data also in the tendency of the relation between the front velocity and the initial temperature, i.e. the front velocity increases if the temperature increases.

6.3. Two-phase expansion tube

This test consists of a 1 m long tube filled with liquid water at atmospheric pressure and with density $\rho_l = 1150\ \mathrm{kg/m^3}$. A weak volume fraction of vapor ($\alpha_v = 0.01$) is initially added to the liquid. The initial discontinuity is set at 0.5 m, the left velocity is -2 m/s and the right velocity is 2 m/s.

In this test the water can not be treated as pure, and only the metastability condition is used to activate the phase transition, i.e. phase transition occurs if the liquid is metastable, i.e. if $T_l > T_{sat}(p_{equi})$. For the computation of $T_{sat}(p_{equi})$ see Appendix C.

This test case requires a small time step to obtain a stable solution (CFL $\approx$ 0.15). When the strong rarefaction are considered a smaller time step is required (CFL $\approx$ 0.03). Here for the sake of comparison we choose to do all computations with CFL = 0.03. The small time here indicates that there is a stiffness coming from the relaxation procedures.

Both procedures of the Gibbs free energy relaxation give the same results, but we consider that the second procedure has a better resolution, thus it is adopted for this test case.

In Fig. 8, we see the solution of this problem without phase transition at $t = 3.2$ ms. The results are obtained by the seven-equation model and are compared with those of the six-equation model, they are completely coinciding. The solution

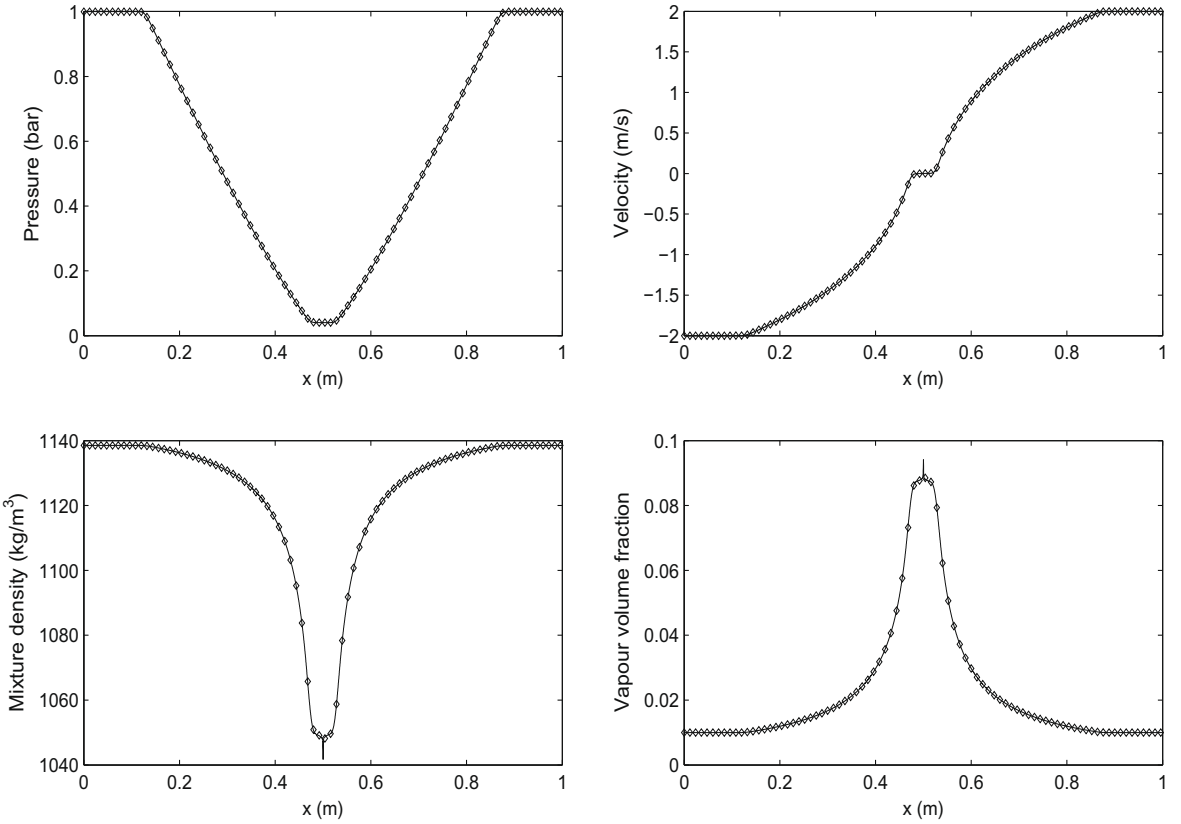

Fig. 8. Water liquid–vapor expansion tube without phase transition, by using the seven-equation model (lines) and six-equation model (symbols). The computations were done with 5000 cells. For the seven-equation model: The CPU time is 14.772 h with 763,550 time steps. For the six-equation model: The CPU time is 7.305 h with 763,726 time steps.

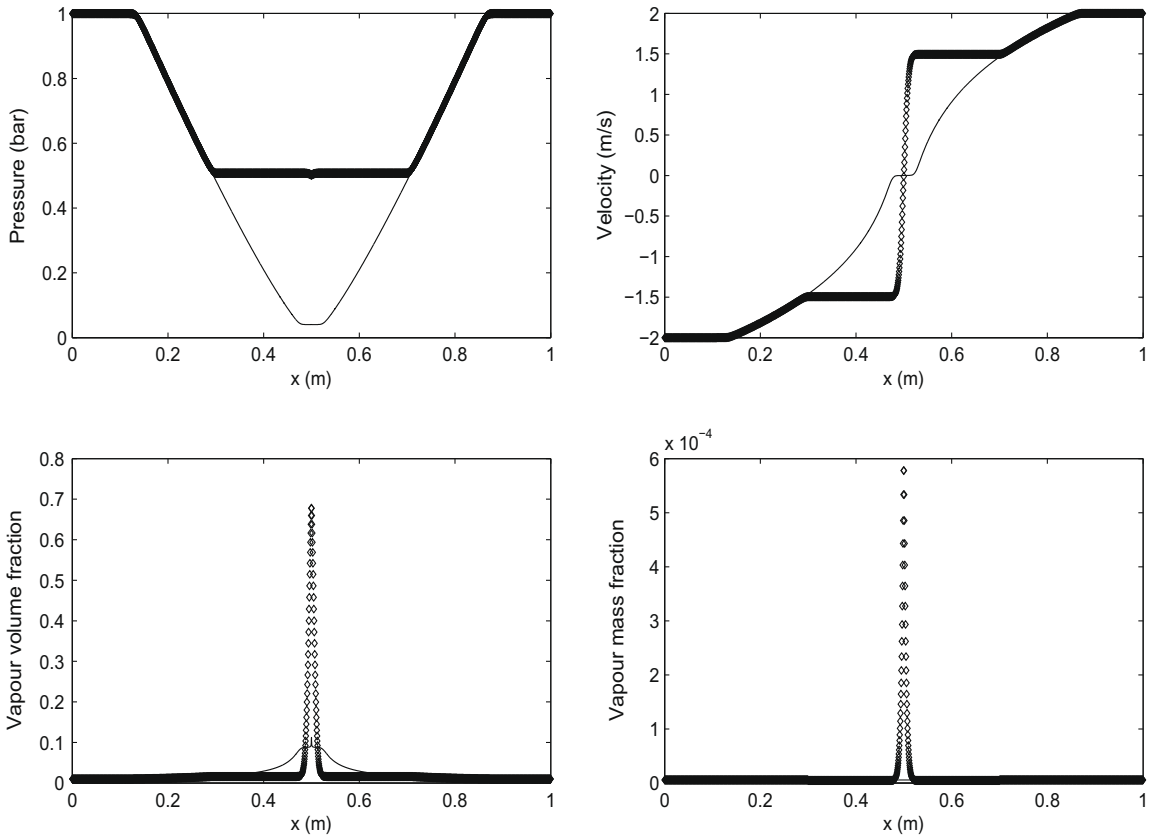

Fig. 9. Water liquid–vapor expansion tube with phase transition at $t = 3.2$ ms, the computed results by the seven-equation model with phase transition (symbols) are compared with the results of the same model without phase transition (lines). The computations were done with 5000 cells. For the model without phase transition: The CPU time is 14.772 h with 763,550 time steps. when the phase transition is included: The CPU time is 18.838 h with 763,550 time steps.

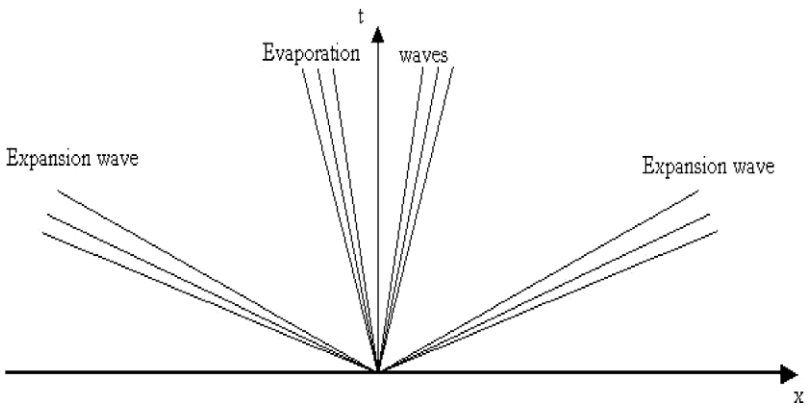

Fig. 10. The waves pattern that correspond to the solutions in Figs. 9 and 11. As shown the evaporation waves are expansion waves.

involves two expansion waves. The vapor volume fraction increases at the center of the domain due to the gas mechanical expansion present in small proportions [33].

The rarefaction waves make the liquid metastable and phase transition has to be added. Fig. 9 presents the solution when the phase transition is involved and is compared with the solution without phase transition at $t = 3.2$ ms. Liquid water is expanded until the saturation pressure is reached (see the pressure graph) then evaporation appears and quite small of vapor is created, for details see [33]. In Fig. 11 a comparison between the results of the seven-equation and the six-equation models is made at the same time, the curves are completely coinciding.

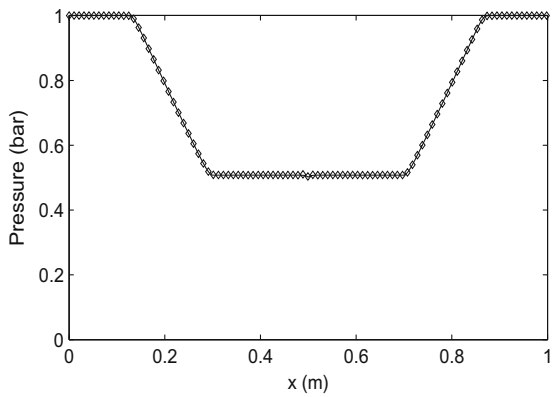

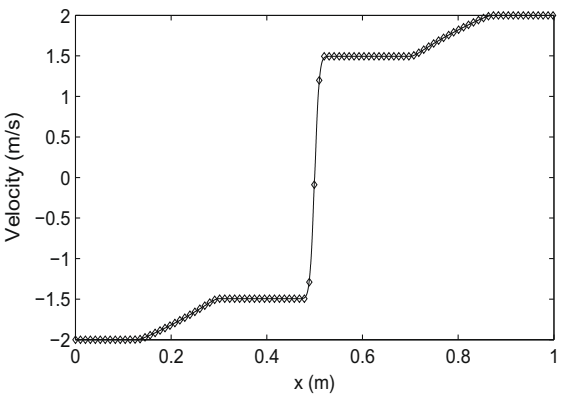

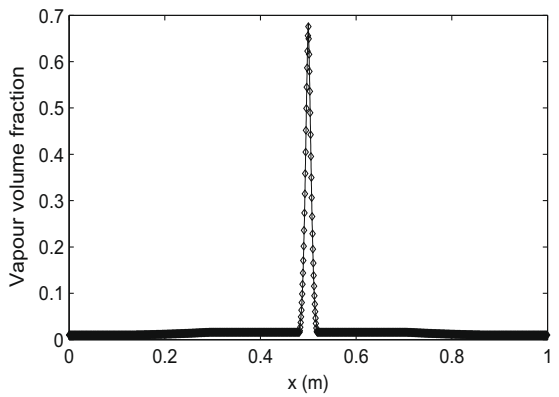

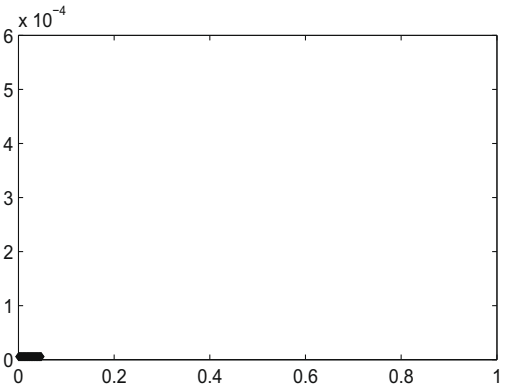

The solution with phase transition, Figs. 9 and 11, is composed of four expansion waves. This is clear if we consider the vapor volume fraction profile on a logarithmic scale as in Fig. 12. Thus the wave pattern is as drawn in Fig. 10. The extra two expansion waves correspond to the evaporation fronts.

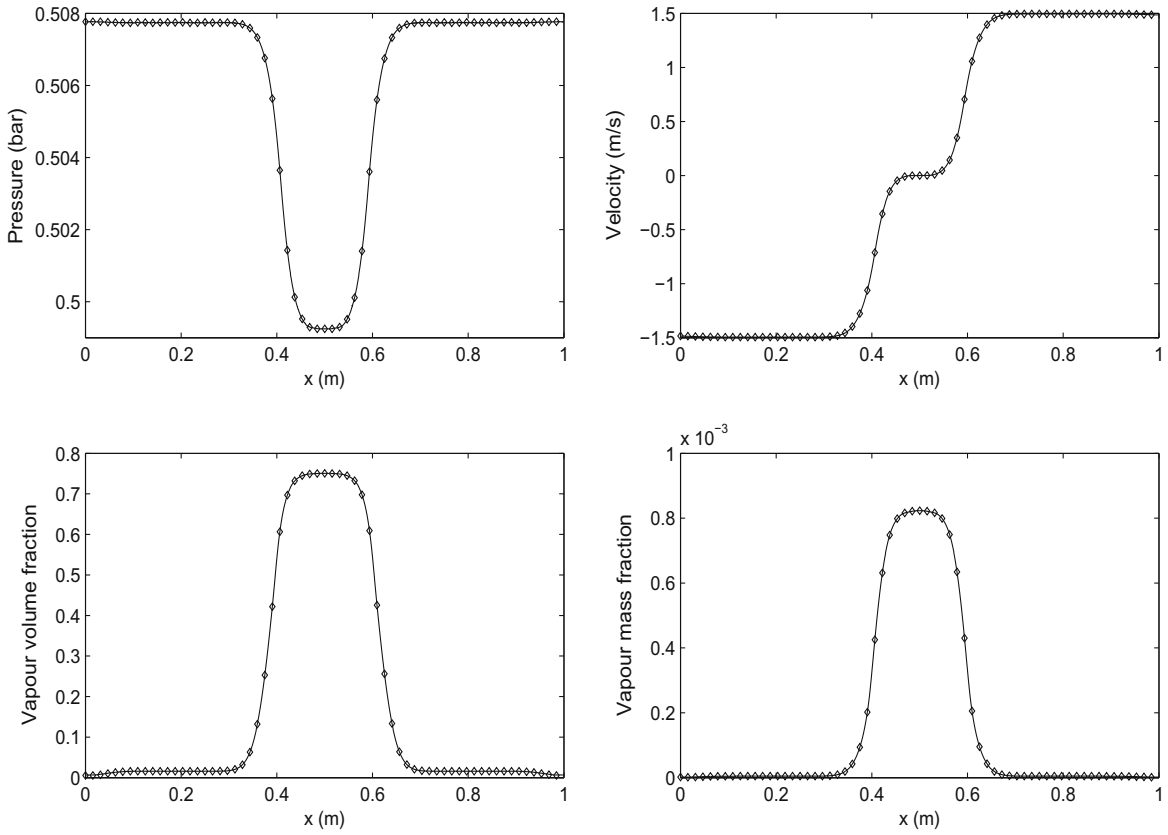

Fig. 13. Water liquid–vapor expansion tube with phase transition at time $t = 59$ ms, by using the seven-equation model (lines) and six-equation model (symbols). The two slow evaporation waves are visible. The computations were done with 3200 cells. For the seven-equation model: The CPU time is 116.078 h with 8,217,444 time steps. For the six-equation model: The CPU time is 99.406 h with 8,217,444 time steps.

If we consider the solution at later time, when $t = 59$ ms as in Fig. 13, the two leading fast expansion waves leave the tube and the two slow evaporation waves are clearly visible. It is clear that these evaporation waves are expansion waves. Also it is clear that the results of the seven-equation model and the six-equation model are completely coinciding.

To see the four expansion waves in one single graph we increase the value of the velocity which means an increase in the rarefaction effects. Under the same conditions except with a velocity -100 m/s on the left and 100 m/s on the right, the four waves are clearly visible as in Fig. 14 at time $t = 1.5$ ms.

When the rarefaction effects become stronger we observe some difficulties. If the same conditions are maintained except the velocity is increased ($\gtrsim 200$ m/s), we see that there are some differences between the results of both models. To consider such difficulty also for the sake of comparsion with the results of Saurel et al. [33], we take the velocity -500 m/s on the left and 500 m/s on the right. The results are shown in Fig. 15 at time $t = 0.58$ ms. There are some differences in the profiles of the pressure and the vapor mass fraction. Moreover there are some oscillations in the curve of the vapor mass fraction. We think that the differences in the results of both models may be related to the approximation of the non-conservative terms and to the fact that in seven-equation model an approximation is used in the velocity relaxation procedure. This may cause some deviation as the difference between the initial velocities is increased.

Under the grid refinement, the differences between the pressure profiles are decreased. They disappear with a very fine grid, as is shown in Fig. 16. But the difference between the vapor mass fraction profiles remains, moreover the oscillations are more pronounced. To understand why the oscillations increase with grid refinement, we consider all variables that are related to the vapor mass fraction $Y_1 = \alpha_1\rho_1/\rho$. We see that as the number of the cells increases the mixture density decreases to a value very close to zero with small oscillations. Also the difference between the mixture density of the two models is reduced. But since the mixture density with low values lies in the denominator of the relation of Y_1, both of the differences and the oscillations in the curves of the vapor mass fraction will be more significant.

Again in this example it is noted that the required CPU time for the six-equation model is smaller than the CPU time that is required for the seven-equation model, in average it is about 66%. In all cases the results of both models coincide except when the difference between the initial velocities increases to a certain value, after that value is reached we observe a small deviation in the results of both models, also some oscillations appear. This problem is partially reduced under grid refinement.

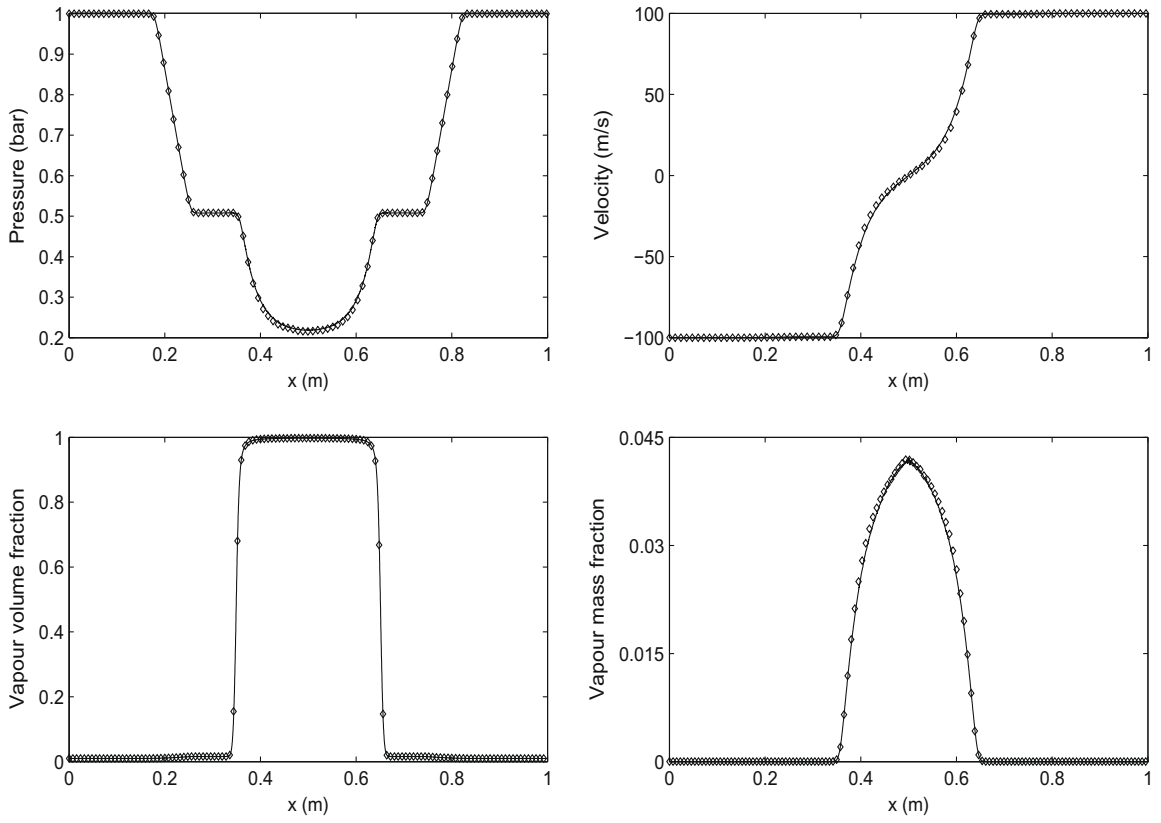

Fig. 14. Water liquid–vapor expansion tube with phase transition and strong rarefaction effects (initial $|u| = 100$ m/s) at time $t = 1.5$ ms. The computations are done with 5000 cells. For the seven-equation model: The CPU time is 8.537 h with 449,836 time steps. For the six-equation model: The CPU time is 5.700 h with 381,778 time steps.

As a result we think that since both models give the same results and also both of them may face similar problems under extreme initial conditions. We think that the six-equation model is to be preferred for practical applications since it is less expensive. Moreover it is easier to modify this model to the multiphase case.

7. Conclusion

In this paper, we modified the seven-equation model for two-phase flows to include the heat and mass transfer through relaxation effects. Depending on the assumption that each property relaxes in a time is considerably different from the other characteristic times, we were able to model the effect of heat and mass transfer by using temperature and Gibbs free energy relaxations. The same ideas are also applied to the six-equation model with a single velocity, which is obtained from the seven-equation model in the limit of zero velocity relaxation time.

A modified Godunov-type method is used to solve the hyperbolic part of each model, while simple relaxation procedures are proposed for the temperature and Gibbs free energy relaxations.

We tested this model on the test problems of Saurel et al. [33]. We were able to see also the extra expansion waves in our results which correspond to the evaporation fronts. Our results are similar to the results of Saurel et al. [33] with few differences.

Computed front velocities in a shock tube at different initial temperatures are compared with experimental ones. A reasonable agreement is achieved.

A comparison between the results of the seven-equation model and the six-equation model was made. Both models almost give the same results, but the six-equation model is less expensive than the seven-equation model and easier to adopt to the multiphase case.

Due to the relaxation processes a stiffness may be encountered during the numerical computations. This requires a smaller time step than is needed for the hydrodynamic system. In particular, if the stiffness comes from the Gibbs free energy relaxation procedure it is possible to use a limitation on the source terms which can be used to find reduced time steps. Then a successive point integration is used to cover the complete hydrodynamic time step. Otherwise small CFL numbers would used and this consumes more computation time. In fact, this point still requires further efforts. For future work, the efficiency

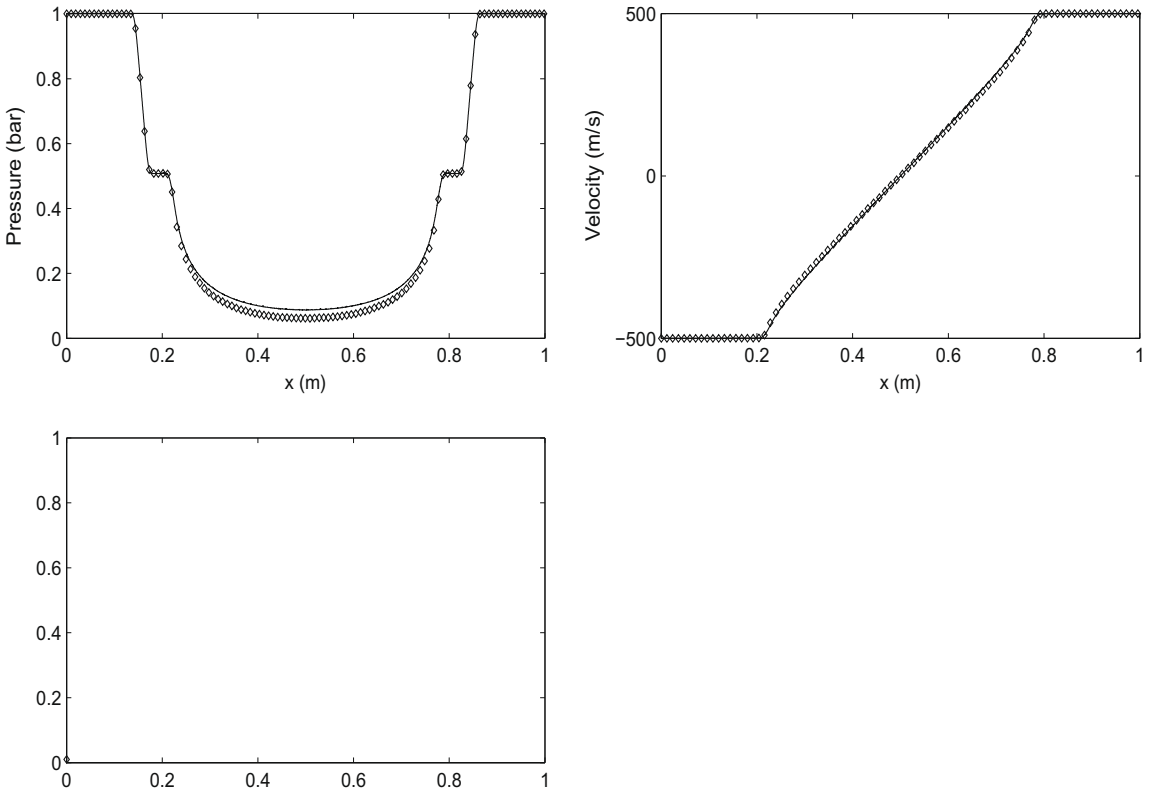

of the numerical method must be improved by using some adaptive discretizations. This will be particularly important when the method is applied to two or three dimensional problems.

We observed that in mixtures under a high difference in the initial velocities there is a small deviation between the results of the seven-equation and six-equation models. This is reduced under grid refinement. We think this deviation is related to the approximation of the non-conservative terms and to some approximation used in velocity relaxation for the seven-equation model. However, to build a specific understanding for this point still more investigations are required. In fact, an extensive convergence study for both models would be very useful for this comparison and further insight into the models. This is a challenging issue for future work.

Appendix A. Mathematical properties of the seven-equation model

In order to investigate the mathematical properties of the model (1), we rewrite it in terms of primitive variables as

$$\frac{\partial \mathbf{W}}{\partial t} + \mathbf{A}\frac{\partial \mathbf{W}}{\partial x} = \mathbf{S} \tag{A.1}$$

where $\mathbf{W} = (\alpha_1, \rho_1, u_1, p_1, \rho_2, u_2, p_2)^T$, the source vector $\mathbf{S}$ represents the non-differential source terms and the matrix $\mathbf{A}$ is given as

$$\mathbf{A} = \begin{bmatrix} u_I & 0 & 0 & 0 & 0 & 0 & 0 \\ \frac{\rho_1}{\alpha_1}(u_1 - u_I) & u_1 & \rho_1 & 0 & 0 & 0 & 0 \\ \frac{p_1 - p_I}{\alpha_1 \rho_1} & 0 & u_1 & \frac{1}{\rho_1} & 0 & 0 & 0 \\ \frac{\rho_1 c_{I,1}^2}{\alpha_1}(u_1 - u_I) & 0 & \rho_1 c_1^2 & u_1 & 0 & 0 & 0 \\ -\frac{\rho_2}{\alpha_2}(u_2 - u_I) & 0 & 0 & 0 & u_2 & \rho_2 & 0 \\ -\frac{p_2 - p_I}{\alpha_2 \rho_2} & 0 & 0 & 0 & 0 & u_2 & \frac{1}{\rho_2} \\ -\frac{\rho_2 c_{I,2}^2}{\alpha_2}(u_2 - u_I) & 0 & 0 & 0 & 0 & \rho_2 c_2^2 & u_2 \end{bmatrix}.$$

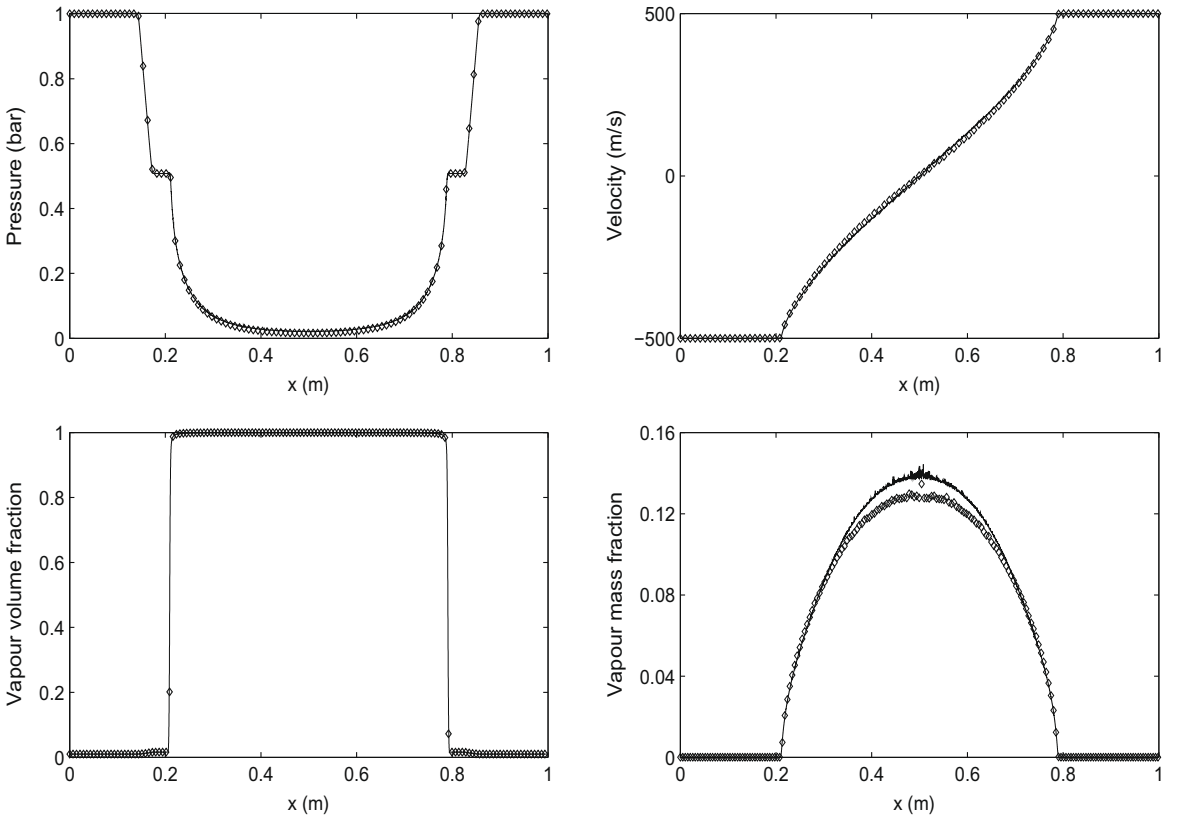

Fig. 16. Water liquid–vapor expansion tube with phase transition and strong rarefaction effects (initial $|u| = 500$ m/s) at time $t = 0.58$ ms. By using the seven-equation model (lines) and six-equation model (symbols). The computations are done with 25,000 cells. For the seven-equation model: The CPU time is 112.393 h with 1,090,545 time steps. For the six-equation model: The CPU time is 85.4813 h with 934,593 time steps.

Where the speed of sound c_k is given in (4) and $c_{I,k}$, *the speed of sound at interface*, is determined by

$$c_{I,k}^2 = \frac{\frac{p_I}{\rho_k^2} - \left(\frac{\partial e_k}{\partial \rho_k}\right)_{p_k}}{\left(\frac{\partial e_k}{\partial p_k}\right)_{\rho_k}}, \quad k = 1, 2. \tag{A.2}$$

The matrix **A** has real eigenvalues that are given by the following expressions

$$\begin{aligned}
&\lambda_1 = u_I,\\
&\lambda_2 = u_1 - c_1, \quad \lambda_3 = u_1, \quad \lambda_4 = u_1 + c_1,\\
&\lambda_5 = u_2 - c_2, \quad \lambda_6 = u_2, \quad \lambda_7 = u_2 + c_2.
\end{aligned}$$

The corresponding right eigenvectors are

$$\mathbf{r}_1 = \begin{bmatrix}
\alpha_1\alpha_2\sigma_1\sigma_2\\
-\alpha_2\sigma_2(\rho_1(\sigma_1 - c_{I,1}^2) + p_1 - p_I)\\
\alpha_2\sigma_2(u_1 - u_I)(p_1 - p_I - \rho_1 c_{I,1}^2)/\rho_1\\
\alpha_2\sigma_2(\rho_1 c_{I,1}^2(u_1 - u_I)^2 - c_1^2(p_1 - p_I))\\
-\alpha_1\sigma_1(\rho_2(c_{I,2}^2 - \sigma_2) - p_2 + p_I)\\
\alpha_1\sigma_1(u_2 - u_I)(-p_2 + p_I + \rho_2 c_{I,2}^2)/\rho_2\\
\alpha_1\sigma_1(-\rho_2 c_{I,2}^2(u_2 - u_I)^2 + c_2^2(p_2 - p_I))
\end{bmatrix}, \tag{A.3}$$

$$\mathbf{r}_2 = \begin{bmatrix} 0 \\ \rho_1 \\ -c_1 \\ \rho_1 c_1^2 \\ 0 \\ 0 \\ 0 \end{bmatrix}, \quad \mathbf{r}_3 = \begin{bmatrix} 0 \\ 1 \\ 0 \\ 0 \\ 0 \\ 0 \\ 0 \end{bmatrix}, \quad \mathbf{r}_4 = \begin{bmatrix} 0 \\ \rho_1 \\ c_1 \\ \rho_1 c_1^2 \\ 0 \\ 0 \\ 0 \end{bmatrix} \tag{A.4}$$

$$\mathbf{r}_5 = \begin{bmatrix} 0 \\ 0 \\ 0 \\ 0 \\ \rho_2 \\ -c_2 \\ \rho_2 c_2^2 \end{bmatrix}, \quad \mathbf{r}_6 = \begin{bmatrix} 0 \\ 0 \\ 0 \\ 0 \\ 1 \\ 0 \\ 0 \end{bmatrix}, \quad \mathbf{r}_7 = \begin{bmatrix} 0 \\ 0 \\ 0 \\ 0 \\ \rho_2 \\ c_2 \\ \rho_2 c_2^2 \end{bmatrix}. \tag{A.5}$$

where

$$\sigma_1 = c_1^2 - (u_1 - u_I)^2, \quad \sigma_2 = c_2^2 - (u_2 - u_I)^2.$$

Thus, the system (1) is strictly hyperbolic except when some of the eigenvalues coincide. Indeed the eigenvectors A.3, A.4 and A.5 become linearly dependent if any one of the conditions

$$\alpha_1 = 0, \quad \alpha_2 = 0, \quad \sigma_1 = 0, \quad \sigma_2 = 0$$

holds. For more details see Andrianov [2].

Consider the Riemann problem for the system (A.1) which is the initial-value problem with initial data of the form

$$\mathbf{W}(x,0) = \begin{cases} \mathbf{W}_L, & x < 0 \\ \mathbf{W}_R, & x > 0. \end{cases}$$

One can show that the characteristic fields associated with λ_1, λ_3 and λ_6 are linearly degenerate, and the 2-, 4-, 5- and 7-fields are genuinely nonlinear. For a proof see Labois [16].

Appendix B. Derivation of the six-equation model from the seven-equation model

This appendix is devoted to the derivation of the six-equation model with heat and mass transfer (74) from the full seven-equation model with heat and mass transfer (64) by the asymptotic limit considering stiff velocity relaxation. We follow the method of Chen et al. [6]. This method is used by Murrone and Guillard [23] in the derivation of the five-equation model from the seven-equation model.

Firstly, we introduce briefly the method of reduction for a system of hyperbolic conservation laws in the presence of stiff relaxation terms using the notations of Murrone and Guillard [23].

Consider a hyperbolic system with stiff source relaxation terms, i.e. consider the following system

$$\frac{\partial \mathbf{W}}{\partial t} + \mathbf{A}(\mathbf{W})\frac{\partial \mathbf{W}}{\partial x} = \frac{\mathbf{R}(\mathbf{W})}{\varepsilon} + \mathbf{S}(\mathbf{W}) \tag{B.1}$$

with $\varepsilon \to 0^+$. The vector $\mathbf{W}$ belongs to Ω, some open subset of $\mathbb{R}^N$.

As $\varepsilon \to 0^+$, the solution of the system (B.1) is expected to be close to the set $\mathfrak{I} \subset \mathbb{R}^N$, where

$$\mathfrak{I} = \{\mathbf{W} \in \mathbb{R}^N; \mathbf{R}(\mathbf{W}) = \mathbf{0}\}.$$

We make use of the following assumption, Murrone and Guillard [23]:

Assumption 1. The set of equations $\mathbf{R}(\mathbf{W}) = 0$ defines a smooth manifold of dimension n, where $0 < n < N$. Moreover, for any $\mathbf{W} \in \mathfrak{I}$ we explicitly know the parameterization M from ω an open subset of $\mathbb{R}^n$ onto V a neighborhood of $\mathbf{W}$ in $\mathfrak{I}$, i.e.

$$M: \ \omega \subset \mathbb{R}^n \to V \subset \mathfrak{I} \subset \mathbb{R}^N,$$
$$\mathbf{w} \to \mathbf{W} = M(\mathbf{w}).$$

Under Assumption 1 the following holds. For any $\mathbf{w} \in \omega$ the Jacobian matrix $dM_{\mathbf{w}}$ is a full rank matrix. Also the column vectors of $dM_{\mathbf{w}}$ form a basis of $\ker(\mathbf{R}'(M(\mathbf{w})))$. For the proof see [23].

Let

$$\mathbf{C} = [dM^1_{\mathbf{w}}, \ldots, dM^n_{\mathbf{w}}, I^1, \ldots, I^{N-n}], \tag{B.2}$$

where $dM^1_{\mathbf{w}}, \ldots, dM^n_{\mathbf{w}}$ are the column vectors of $dM_{\mathbf{w}}$ and $I^1, \ldots, I^{N-n}$ are a basis of the range $\mathrm{rng}(\mathbf{R}'(M(\mathbf{w})))$ of $\mathbf{R}'(M(\mathbf{w}))$. The matrix (B.2) is invertible, let $\mathbf{B}$ be the matrix composed of the first n rows of the inverse of the matrix $\mathbf{C}$. Then we have the following results:

$$\mathbf{B} \cdot dM_{\mathbf{w}} = \mathbf{I}_{n\times n}, \text{the identity matrix} \tag{B.3a}$$

$$\mathbf{B} \cdot \mathbf{R}'(M(\mathbf{w})) = 0. \tag{B.3b}$$

For proof see the same Ref. [23].

Decompose the state vector $\mathbf{W}$ as

$$\mathbf{W} = M(\mathbf{w}) + \varepsilon \mathbf{V}, \tag{B.4}$$

where $\mathbf{V}$ is a small perturbation around the state vector $M(\mathbf{w})$.

To obtain the reduced model we use the expression (B.4) in the system (B.1) and get

$$\frac{\partial M(\mathbf{w})}{\partial t} + \mathbf{A}(M(\mathbf{w}))\frac{\partial M(\mathbf{w})}{\partial x} - \mathbf{R}'(M(\mathbf{w})) \cdot \mathbf{V} = \mathbf{S}(M(\mathbf{w})) + O(\varepsilon). \tag{B.5}$$

Multiplying (B.5) by $\mathbf{B}$, using (B.3) and neglecting the terms of order ε, we obtain the reduced model of the system (B.1)

$$\frac{\partial \mathbf{w}}{\partial t} + \mathbf{B} \cdot \mathbf{A}(M(\mathbf{w})) \cdot dM_{\mathbf{w}} \frac{\partial \mathbf{w}}{\partial x} = \mathbf{B} \cdot \mathbf{S}(M(\mathbf{w})). \tag{B.6}$$

Now, we apply the above method for the reduction by using the asymptotic limit on the seven-equation model assuming a stiff velocity relaxation.

Take the vector of primitive variables as $\mathbf{W} = (\alpha_1, \rho_1, \rho_2, u_1, u_2, p_1, p_2)$, and write the seven-equation model (64) accompanied with all relaxation terms in the form (B.1). In this case, the source vector $\frac{\mathbf{R}(\mathbf{W})}{\varepsilon}$ consists of the velocity relaxation terms which is stiff, i.e. $\lambda = \frac{1}{\varepsilon}$, where $\varepsilon \to 0^+$. While the source vector $\mathbf{S}(\mathbf{W})$ is decomposed as

$$\mathbf{S}(\mathbf{W}) = \mathbf{S}_P(\mathbf{W}) + \mathbf{S}_Q(\mathbf{W}) + \mathbf{S}_m(\mathbf{W}).$$

The matrix $\mathbf{A}(\mathbf{W})$ and the source vectors can be given as

$$\mathbf{A}(\mathbf{W}) = \begin{bmatrix} u_I & 0 & 0 & 0 & 0 & 0 & 0 \\ -\frac{\rho_1}{\alpha_1}(u_I - u_1) & u_1 & 0 & \rho_1 & 0 & 0 & 0 \\ \frac{\rho_2}{\alpha_2}(u_I - u_2) & 0 & u_2 & 0 & \rho_2 & 0 & 0 \\ -\frac{p_I - p_1}{\alpha_1 \rho_1} & 0 & 0 & u_1 & 0 & \frac{1}{\rho_1} & 0 \\ \frac{p_I - p_2}{\alpha_2 \rho_2} & 0 & 0 & 0 & u_2 & 0 & \frac{1}{\rho_2} \\ -\frac{\Gamma_1}{\alpha_1}\left[p_I - \rho_1^2\left(\frac{\partial e_1}{\partial \rho_1}\right)_{p_1}\right](u_I - u_1) & 0 & 0 & \rho_1 c_1^2 & 0 & u_1 & 0 \\ \frac{\Gamma_2}{\alpha_2}\left[p_I - \rho_2^2\left(\frac{\partial e_2}{\partial \rho_2}\right)_{p_2}\right](u_I - u_2) & 0 & 0 & 0 & \rho_2 c_2^2 & 0 & u_2 \end{bmatrix},$$

$$\frac{\mathbf{R}(\mathbf{W})}{\varepsilon} = \begin{bmatrix} 0 \\ 0 \\ 0 \\ \frac{\lambda}{\alpha_1 \rho_1}(u_2 - u_1) \\ -\frac{\lambda}{\alpha_2 \rho_2}(u_2 - u_1) \\ \lambda \frac{\Gamma_1}{\alpha_1}(u_I - u_1)(u_2 - u_1) \\ -\lambda \frac{\Gamma_2}{\alpha_2}(u_I - u_2)(u_2 - u_1) \end{bmatrix},$$

$$\mathbf{S}_P(\mathbf{W}) = \begin{bmatrix} \mu(p_1 - p_2) \\ \mu \frac{\rho_1}{\alpha_1}(p_2 - p_1) \\ -\mu \frac{\rho_2}{\alpha_2}(p_2 - p_1) \\ 0 \\ 0 \\ \mu \frac{\Gamma_1}{\alpha_1}\left[p_I - \rho_1^2\left(\frac{\partial e_1}{\partial \rho_1}\right)_{p_1}\right](p_2 - p_1) \\ -\mu \frac{\Gamma_2}{\alpha_2}\left[p_I - \rho_2^2\left(\frac{\partial e_2}{\partial \rho_2}\right)_{p_2}\right](p_2 - p_1) \end{bmatrix}, \quad \mathbf{S}_Q(\mathbf{W}) = \begin{bmatrix} \frac{1}{\kappa} Q \\ -\frac{\rho_1}{\alpha_1 \kappa} Q \\ \frac{\rho_2}{\alpha_2 \kappa} Q \\ 0 \\ 0 \\ -\frac{\rho_1 c_1^2}{\alpha_1 \kappa} Q + \frac{\Gamma_1}{\alpha_1}(1 + \frac{p_1}{\kappa}) Q \\ \frac{\rho_2 c_2^2}{\alpha_2 \kappa} Q - \frac{\Gamma_2}{\alpha_2}(1 + \frac{p_2}{\kappa}) Q \end{bmatrix},$$

$$\mathbf{S}_m(\mathbf{W}) = \begin{bmatrix} \frac{1}{\varrho}\dot{m} \\ \frac{1}{\alpha_1}(1-\frac{\rho_1}{\varrho})\dot{m} \\ -\frac{1}{\alpha_2}(1-\frac{\rho_2}{\varrho})\dot{m} \\ \frac{1}{\alpha_1\rho_1}(u_I-u_1)\dot{m} \\ -\frac{1}{\alpha_2\rho_2}(u_I-u_2)\dot{m} \\ \frac{c_1^2}{\alpha_1}(1-\frac{\rho_1}{\varrho})\dot{m} + \frac{\Gamma_1}{\alpha_1}\left[(e_i-e_1)+\frac{(u_I-u_1)^2}{2}-\frac{p_1}{\rho_1}(1-\frac{\rho_1}{\varrho})\right]\dot{m} \\ -\frac{c_2^2}{\alpha_2}(1-\frac{\rho_2}{\varrho})\dot{m} - \frac{\Gamma_2}{\alpha_2}\left[(e_i-e_2)+\frac{(u_I-u_2)^2}{2}-\frac{p_2}{\rho_2}(1-\frac{\rho_2}{\varrho})\right]\dot{m} \end{bmatrix}.$$

Where Γ_k is given in (31).

The limit of zero velocity relaxation time gives a single velocity, i.e. $u_1 = u_2 = u$. Thus the vector of the primitive variables for the reduced model is

$$\mathbf{w} = (\alpha_1, \rho_1, \rho_2, u, p_1, p_2)^T.$$

So $M(\mathbf{w})$ is defined as

$$M : \mathbf{w} \to M(\mathbf{w}) = (\alpha_1, \rho_1, \rho_2, u, u, p_1, p_2)^T. \tag{B.7}$$

Then the Jacobian matrix of the transformation (B.7) is given as

$$dM_{\mathbf{w}} = \begin{bmatrix} 1 & 0 & 0 & 0 & 0 & 0 \\ 0 & 1 & 0 & 0 & 0 & 0 \\ 0 & 0 & 1 & 0 & 0 & 0 \\ 0 & 0 & 0 & 1 & 0 & 0 \\ 0 & 0 & 0 & 1 & 0 & 0 \\ 0 & 0 & 0 & 0 & 1 & 0 \\ 0 & 0 & 0 & 0 & 0 & 1 \end{bmatrix}. \tag{B.8}$$

It is easy to see that the Jacobian matrix $\mathbf{R}'$ evaluated on the transformation is given as

$$\mathbf{R}'(M(\mathbf{w})) = \begin{bmatrix} 0 & 0 & 0 & 0 & 0 & 0 & 0 \\ 0 & 0 & 0 & 0 & 0 & 0 & 0 \\ 0 & 0 & 0 & 0 & 0 & 0 & 0 \\ 0 & 0 & 0 & -\frac{1}{\alpha_1\rho_1} & \frac{1}{\alpha_1\rho_1} & 0 & 0 \\ 0 & 0 & 0 & \frac{1}{\alpha_2\rho_2} & -\frac{1}{\alpha_2\rho_2} & 0 & 0 \\ 0 & 0 & 0 & 0 & 0 & 0 & 0 \\ 0 & 0 & 0 & 0 & 0 & 0 & 0 \end{bmatrix}.$$

Obviously, the basis of $\mathrm{rng}(\mathbf{R}'(M(\mathbf{w})))$ is

$$I^1 = \begin{bmatrix} 0 \\ 0 \\ 0 \\ -\frac{1}{\alpha_1\rho_1} \\ \frac{1}{\alpha_2\rho_2} \\ 0 \\ 0 \end{bmatrix}. \tag{B.9}$$

From (B.8) and (B.9) we can find the matrix $\mathbf{C}$, then we can find the matrix $\mathbf{B}$

$$\mathbf{B} = \begin{bmatrix} 1 & 0 & 0 & 0 & 0 & 0 & 0 \\ 0 & 1 & 0 & 0 & 0 & 0 & 0 \\ 0 & 0 & 1 & 0 & 0 & 0 & 0 \\ 0 & 0 & 0 & \frac{\alpha_1\rho_1}{\rho} & \frac{\alpha_2\rho_2}{\rho} & 0 & 0 \\ 0 & 0 & 0 & 0 & 0 & 1 & 0 \\ 0 & 0 & 0 & 0 & 0 & 0 & 1 \end{bmatrix}.$$

By using the matrix **B** together with the above matrices we can find the reduced model as in (B.6). Thus the reduced model in primitive variables is given as

$$\frac{\partial \alpha_1}{\partial t} + u\frac{\partial \alpha_1}{\partial x} = \mu(p_1 - p_2) + \frac{1}{\kappa}Q + \frac{1}{\varrho}\dot{m}, \tag{B.10a}$$

$$\frac{\partial \rho_1}{\partial t} + u\frac{\partial \rho_1}{\partial x} + \rho_1\frac{\partial u}{\partial x} = \mu\frac{\rho_1}{\alpha_1}(p_2 - p_1) - \frac{\rho_1}{\alpha_1\kappa}Q + \frac{1}{\alpha_1}\left(1 - \frac{\rho_1}{\varrho}\right)\dot{m}, \tag{B.10b}$$

$$\frac{\partial \rho_2}{\partial t} + u\frac{\partial \rho_2}{\partial x} + \rho_2\frac{\partial u}{\partial x} = -\mu\frac{\rho_2}{\alpha_2}(p_2 - p_1) + \frac{\rho_2}{\alpha_2\kappa}Q - \frac{1}{\alpha_2}\left(1 - \frac{\rho_2}{\varrho}\right)\dot{m}, \tag{B.10c}$$

$$\frac{\partial u}{\partial t} + u\frac{\partial u}{\partial x} + \frac{(p_1 - p_2)}{\rho}\frac{\partial \alpha_1}{\partial x} + \frac{\alpha_1}{\rho}\frac{\partial p_1}{\partial x} + \frac{\alpha_2}{\rho}\frac{\partial p_2}{\partial x} = 0, \tag{B.10d}$$

$$\begin{aligned}\frac{\partial p_1}{\partial t} + u\frac{\partial p_1}{\partial x} + \rho_1 c_1^2\frac{\partial u}{\partial x} &= \mu\frac{\Gamma_1}{\alpha_1}\left[p_I - \rho_1^2\left(\frac{\partial e_1}{\partial \rho_1}\right)_{p_1}\right](p_2 - p_1) - \frac{\rho_1 c_1^2}{\alpha_1\kappa}Q + \frac{\Gamma_1}{\alpha_1}\left(1 + \frac{p_1}{\kappa}\right)Q \\ &\quad + \frac{c_1^2}{\alpha_1}\left(1 - \frac{\rho_1}{\varrho}\right)\dot{m} + \frac{\Gamma_1}{\alpha_1}\left[(e_i - e_1) - \frac{p_1}{\rho_1}\left(1 - \frac{\rho_1}{\varrho}\right)\right]\dot{m},\end{aligned} \tag{B.10e}$$

$$\begin{aligned}\frac{\partial p_2}{\partial t} + u\frac{\partial p_2}{\partial x} + \rho_2 c_2^2\frac{\partial u}{\partial x} &= -\mu\frac{\Gamma_2}{\alpha_2}\left[p_I - \rho_2^2\left(\frac{\partial e_2}{\partial \rho_2}\right)_{p_2}\right](p_2 - p_1) + \frac{\rho_2 c_2^2}{\alpha_2\kappa}Q - \frac{\Gamma_2}{\alpha_2}\left(1 + \frac{p_2}{\kappa}\right)Q \\ &\quad - \frac{c_2^2}{\alpha_2}\left(1 - \frac{\rho_2}{\varrho}\right)\dot{m} - \frac{\Gamma_2}{\alpha_2}\left[(e_i - e_2) - \frac{p_2}{\rho_2}\left(1 - \frac{\rho_2}{\varrho}\right)\right]\dot{m},\end{aligned} \tag{B.10f}$$

where $\rho = \alpha_1\rho_1 + \alpha_2\rho_2$.

Using Eqs. (B.10b) and (B.10c) with (B.10a), we obtain

$$\frac{\partial \alpha_1\rho_1}{\partial t} + \frac{\partial(\alpha_1\rho_1 u)}{\partial x} = \dot{m},$$
$$\frac{\partial \alpha_2\rho_2}{\partial t} + \frac{\partial(\alpha_2\rho_2 u)}{\partial x} = -\dot{m}.$$

Using these equations with (B.10d), we get

$$\frac{\partial \rho u}{\partial t} + \frac{\partial(\rho u^2 + \alpha_1 p_1 + \alpha_2 p_2)}{\partial x} = 0.$$

The internal energy of each phase can be written as a function of the phase density and pressure, i.e. $e_k = e_k(\rho_k, p_k), k = 1, 2$. Then we obtain the following expression for the differential de_k

$$de_k = \left(\frac{\partial e_k}{\partial \rho_k}\right)_{p_k} d\rho_k + \left(\frac{\partial e_k}{\partial p_k}\right)_{\rho_k} dp_k. \tag{B.11}$$

With the help of this equation and with the equations of the system (B.10), we obtain the following equations for the internal energies

$$\frac{\partial \alpha_1\rho_1 e_1}{\partial t} + \frac{\partial \alpha_1\rho_1 e_1 u}{\partial x} + \alpha_1 p_1\frac{\partial u}{\partial x} = \mu p_I(p_2 - p_1) + Q + e_i\dot{m},$$
$$\frac{\partial \alpha_2\rho_2 e_2}{\partial t} + \frac{\partial \alpha_2\rho_2 e_2 u}{\partial x} + \alpha_2 p_2\frac{\partial u}{\partial x} = -\mu p_I(p_2 - p_1) - Q - e_i\dot{m}.$$

Thus the whole model can be written as in (74).

Appendix C. Determination of $T_{sat}(p_{equi})$

The metastable condition $T_k > T_{sat}(p_{equi})$ is used to activate the phase transition. In this appendix we consider the computation of the curve $T = T_{sat}(p)$.

Simply we use the same idea of [21,33] that at thermodynamic equilibrium the Gibbs free energies are equal, and this equality provides a direct relation between the saturation pressure and temperature.

Using the SG-EOS (5) the Gibbs free energy g_k is expressed as

$$g_k = (\gamma_k C_{vk} - q_k')T_k - T_k C_{vk}\ln\frac{T_k^{\gamma_k}}{(p_k + \pi_k)^{(\gamma_k - 1)}} + q_k.$$

At the saturation curve we have an equilibrium pressure p, an equilibrium temperature T and by the equality of the two Gibbs free energies g_1 and g_2 we have

$$(\gamma_1 C_{v1} - q_1')T - TC_{v1}\ln\frac{T^{\gamma_1}}{(p+\pi_1)^{(\gamma_1-1)}} + q_1 = (\gamma_2 C_{v2} - q_2')T - TC_{v2}\ln\frac{T^{\gamma_2}}{(p+\pi_2)^{(\gamma_2-1)}} + q_2.$$

This equation is nonlinear and can be solved by any iterative technique to find the saturation temperature in terms of the saturation pressure.

References

[1] R. Abgrall, How to prevent pressure oscillations in multicomponent flow calculations: a quasi conservative approach, J. Comput. Phys. 125 (1) (1996) 150–160.
[2] N. Andrianov, Analytical and Numerical Investigation of Two-phase Flows, Ph.D. Thesis, Otto-von-Guericke University, 2003.
[3] N. Andrianov, R. Saurel, G. Warnecke, A simple method for compressible multiphase mixtures and interfaces, Int. J. Numer. Methods Fluids 41 (2003) 109–131.
[4] M.R. Baer, J.W. Nunziato, A two-phase mixture theory for the deflagration-to-detonation transition (DDT) in reactive granular materials, Int. J. Multiphase Flows 12 (1986) 861–889.
[5] Z. Bilicki, R. Kwidzinski, SA. Mohammadein, An estimation of a relaxation time of heat and mass exchange in the liquid-vapour bubble flow, Int. J. Heat Mass Transfer 39 (4) (1996) 753759.
[6] G.Q. Chen, C.D. Levermore, T.P. Liu, Hyperbolic conservation laws with stiff relaxation terms and entropy, Commun. Pure Appl. Math. 47 (1994) 787–830.
[7] A. Chinnayya, E. Daniel, R. Saurel, Modelling detonation waves in heterogeneous energetic materials, J. Comput. Phys. 196 (2) (2004) 490–538.
[8] S.F. Davis, Simplified second-order Godunov-type methods, SIAM J. Sci. Statist. Comput. 9 (1988) 445–473.
[9] D.A. Drew, Mathematical modeling of two-phase flow, Ann. Rev. Fluid Mech. 15 (1983) 261–291.
[10] D.A. Drew, S.L. Passman, Theory of multicomponent fluids, Applied Mathematical Sciences, vol. 135, Springer, New York, 1998.
[11] P. Embid, M. Baer, Mathematical analysis of a two-phase continuum mixture theory, Continuum Mech. Thermodyn. 4 (1992) 279–312.
[12] T. Gallouët, J.M. Masella, Un schéma de Godunov approaché, Comptes Rendus Académie des Sciences Paris, Série I 323 (1996) 7784.
[13] H. Guillard, M. Labois, Numerical modeling of compressible two-phase flows, in: P. Wesseling, E. Onate, J. Priaux (Ed.), European Conference on Computational Fluid Dynamics ECCOMAS CFD, 2006.
[14] M. Ishii, T. Hibiki, Thermo Fluid Dynamics of Two-phase Flow, Springer Science + Business Media, Inc., 2006.
[15] A.K. Kapila, R. Menikoff, J.B. Bdzil, S.F. Son, D.S. Stewart, Two-phase modelling of DDT in granular materials: reduced equations, Phys. Fluids 13 (2001) 3002–3024.
[16] M. Labois, Modélisation des déséquilibres mécaniques pour les écoulements diphasiques: approches par relaxation et par modèle réduit, Ph.D. Thesis, Université de Provence – Aix-Marseille I, 2008.
[17] M.H. Lallemand, A. Chinnayya, O. Le Metayer, Pressure relaxation procedures for multiphase compressible flows, Int. J. Numer. Methods Fluids 49 (1) (2005) 1–56.
[18] M.H. Lallemand, R. Saurel, Pressure Relaxation Procedures for Multi-phase Compressible Flows, Technical Report 4038, INRIA, 2000.
[19] R. Menikoff, B.J. Plohr, The Riemann problem for fluid flow of real materials, Rev. Mod. Phys. 61 (1) (1989) 75–130.
[20] O. Le Metayer, J. Massoni, R. Saurel, Elaborating equations of state of a liquid and its vapor for two-phase flow models (in French), Int. J. Therm. Sci. 43 (3) (2004) 265276.
[21] O. Le Metayer, J. Massoni, R. Saurel, Modelling evaporation fronts with reactive Riemann solvers, J. Comput. Phys. 205 (2005) 567–610.
[22] I. Müller, W.H. Müller, Fundamentals of Thermodynamics and Applications: With Historical Annotations and Many Citations from Avogadro to Zermelo, Springer-Verlag, Berlin Heidelberg, 2009.
[23] A. Murrone, H. Guillard, A five-equation reduced model for compressible two-phase flow problems, J. Comput. Phys. 202 (2) (2005) 664–698.
[24] F. Petitpas, E. Franquet, R. Saurel, O. Le Metayer, A relaxation–projection method for compressible flows. Part II: artificial heat exchanges for multiphase shocks, J. Comput. Phys. Arch. 225 (2) (2007) 2214–2248.
[25] F. Petitpas, J. Massoni, R. Saurel, E. Lapebie, L. Munier, Diffuse interface models for high speed cavitating underwater systems, Int. J. Multiphase Flows 35 (8) (2009) 747–759.
[26] F. Petitpas, R. Saurel, E. Franquet, A. Chinnayya, Modelling detonation waves in condensed materials: multiphase CJ conditions and multidimensional computations, Shock waves 19 (2009) 377–401.
[27] R. Saurel, R. Abgrall, A multiphase Godunov method for compressbile multifluid and multiphase flows, J. Comput. Phys. 150 (2) (1999) 425–467.
[28] R. Saurel, R. Abgrall, A simple method for compressible multifluid flows, SIAM J. Sci. Comput. 21 (1999) 1115–1145.
[29] R. Saurel, E. Franquet, E. Daniel, O. Le Metayer, A relaxation–projection method for compressible flows. Part I: the numerical equation of state for the Euler equations, J. Comput. Phys. 223 (2) (2007) 822–845.
[30] R. Saurel, S. Gavrilyuk, F. Renaud, A multiphase model with internal degree of freedom, application to shock–bubble interaction, J. Fluid Mech. 495 (2003) 283–321.
[31] R. Saurel, O. Le Metayer, A multiphase model for interfaces, shocks, detonation waves and cavitation, J. Fluid Mech. 431 (2001) 239–271.
[32] R. Saurel, O. Le Metayer, J. Massoni, S. Gavrilyuk, Shock jump relations for multiphase mixtures with stiff mechanical properties, Shock Waves 16 (2007) 209–232.
[33] R. Saurel, F. Petitpas, R. Abgrall, Modelling phase transition in metastable liquids: application to cavitating and flashing flows, J. Fluid Mech. 607 (2008) 313–350.
[34] R. Saurel, F. Petitpas, R.A. Berry, Simple and efficient relaxation methods for interfaces separating compressible fluids, cavitating flows and shocks in multiphase mixtures, J. Comput. Phys. 228 (5) (2009) 1678–1712.
[35] J.R. Simões-Moreira, Adiabatic Evaporation Waves, Ph.D. Thesis, Rensselaer Polytechnic Institute, 1994.
[36] J.R. Simões-Moreira, J.E. Shepherd, Evaporation waves in superheated dodecane, J. Fluid Mech. 382 (1999) 63–86.
[37] G. Strang, On the construction and comparison of difference schemes, SIAM J. Numer. Anal. 5 (1968) 506–517.
[38] E.F. Toro, Riemann Solvers and Numerical Methods for Fluid Dynamics, Springer, Berlin, 1999.